

STUDY OF BUCKLING BEHAVIOR OF DRYING COLLOIDAL DROPLET

M.Tech. Thesis

by

PANKAJ KUMAR BASER



**DEPARTMENT OF MECHANICAL ENGINEERING
INDIAN INSTITUTE OF TECHNOLOGY
INDORE**

JUNE 2023

STUDY OF BUCKLING BEHAVIOR OF DRYING COLLOIDAL DROPLET

A THESIS

*Submitted in partial fulfillment of the
requirements for the award of the degree*

of

Master of Technology

by

PANKAJ KUMAR BASER



**DEPARTMENT OF MECHANICAL ENGINEERING
INDIAN INSTITUTE OF TECHNOLOGY**

INDORE

JUNE 2023

CANDIDATE'S DECLARATION

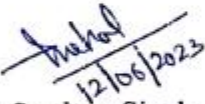
I hereby certify that the work which is being presented in the thesis entitled **STUDY OF BUCKLING BEHAVIOR OF DRYING COLLOIDAL DROPLET** in the partial fulfillment of the requirements for the award of the degree of **MASTER OF TECHNOLOGY** and submitted in the **DISCIPLINE OF MECHANICAL ENGINEERING, Indian Institute of Technology Indore**, is an authentic record of my own work carried out during the time period from **AUGUST 2021 to JUNE 2023** under the supervision of **Dr. Sandeep Singh, Assistant Professor** and **Dr. Ankur Miglani, Assistant Professor**.

The matter presented in this thesis has not been submitted by me for the award of any other degree of this or any other institute.



Pankaj Kumar Baser

This is to certify that the above statement made by the candidate is correct to the best of my/our knowledge.

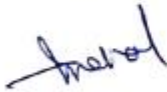


Dr. Sandeep Singh



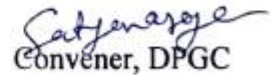
Dr. Ankur Miglani

Pankaj Kumar Baser has successfully given his M. Tech. Oral Examination held on **25 May 2023**.



Signature(s) of Supervisor(s) of M. Tech. thesis

Date: 12/06/2023



Convener, DPGC

Date: 16/06/2023



Signature of PSPC Member #1

Dr. Indrasen Singh

Date:



Signature of PSPC Member #2

Dr. Ranveer Singh

Date: 13/06/2023

ACKNOWLEDGEMENTS

I would like to express my deep gratitude primarily to my respected supervisors, Dr. Sandeep Singh, and Dr. Ankur Miglani, for their expert guidance and support throughout my two-year journey in pursuing a Master of Technology in Mechanical System Design. I consider myself fortunate to have advisors who consistently motivated me and offered invaluable assistance, leading up to the successful completion of this work. I also extend my appreciation to PSPC members, Dr. Indrasen Singh, and Dr. Ranveer Singh, for their feedback and suggestions that contributed to the advancement of this project.

I acknowledge Defence Research and Development Organization (DRDO) for sponsoring my M.Tech. under Research and Training scheme. I am also grateful to my Technology Director, Shri B. Veera Sekhar for granting me permission to pursue M. Tech. amid number of project responsibilities.

I also would like to extend a special acknowledgment to Mr. Janmejy (Ph.D. Scholar) for his invaluable assistance in conducting the experiment, as well as to Mr. Akash Raikwar (Ph.D. Scholar) and Mr. Ashwani Yadav (Ph.D. Scholar) for their unwavering moral support and the conducive environment they created, which greatly contributed to the successful completion of this project.

I want to express my sincere appreciation to all individuals who have provided any assistance, whether through direct or indirect means, throughout the course of this project.

(Pankaj Kumar Baser)

**Dedicated to my family members and my beloved
wife, for their unwavering love and care throughout
this journey**

Abstract

Stability behaviour of drying colloidal droplet for fast drying condition ($Pe > 1$) is investigated according to theory of shallow shell. To capture the local buckling behaviour of colloidal droplet, a small segment from full spherical shape is considered for modelling through shallow shell theory. Theoretical studies are carried out considering two different segments, for first case square segment is considered assuming segment to be pin jointed with rest of the shell structure and for second case circular segment is considered assuming segment to be clamped with rest of the shell structure. The closed form relation for lower critical buckling pressure and critical relation between droplet radius and particle size as well in terms of shell parameter such as particle size, particle packing volume fraction, particle coordination number and elastic properties of particles are formulated. Theoretical outcome of the study compared with experimental data.

The relations for size of the dent and dent amplitude in terms of colloid particle size are also obtained. The results presented here could help in altering the morphology of drying droplet in numerous applications of spray drying process.

TABLE OF CONTENTS

LIST OF FIGURES	V
LIST OF TABLES	VIII
NOMENCLATURE	IX
1. Introduction	1
1.1 Overview	1
1.2 Buckling of Colloidal Shell	1
1.3 Applications	3
1.4 Significance and Objective	3
1.5 Thesis Outline	4
2. Literature Review	5
3. Theory of Shallow Shell for Colloidal Droplet	8
3.1. Governing Differential Equations of Shell Theory	8
3.2. Parameters in Polar Coordinates	13
4. Equivalent Elastic Parameter	15
5. Stability Analysis of Colloidal Droplet	16
5.1. Stability Analysis of Spherical Shell Considering Square Segment	16
5.2. Stability Analysis of Spherical Shell Considering Circular Segment	25
6. Experimental Methods	38
6.1. Experimental Techniques to Create Spherical Droplet	38
6.1.1. Sessile droplet	38
6.1.2. Free flying droplet	39
6.1.3. Pendent droplet	39
6.2. Preparation of Aqueous Suspension of Colloid Particles	39
6.3. Experimental Setup and Procedure	40
7. Results and Discussion	43
8. Conclusion and Future Scope	49
REFERENCES	50

LIST OF FIGURES

Figure 1.1	Sessile droplet of colloidal solution at various stages of evaporation.	2
Figure 1.2	Snap through buckling of thin-walled table tennis ball.	2
Figure 1.3	Dried corn kernels and peas.	2
Figure 2.1	Effect of Peclet number (Pe) on morphology of resultant shell from desiccation of colloidal droplet.	6
Figure 2.2	Schematic of a sessile droplet drying at a high evaporation rate and the pressure variation in the droplet.	7
Figure 3.1	The schematic shows the stress resultant and stress couple and their direction acting on small element characterizing state of stress of the shell element. Note that all stress resultants and stress couples are acting at middle surface of the shell. z direction is towards the center of curvature the shell.	10
Figure 3.2	The schematic shows the stress resultant and stress couple and their direction acting on small element characterizing state of stress of the shell element. Note that all stress resultants and stress couples are acting at middle surface of the shell. z direction is towards the centre of curvature of the shell.	10
Figure 5.1	Schematic of a spherical shell and a small square segment of size (a) considered for stability analysis. Boundary of shell segment is assumed to be pin connected with rest of the shell.	17
Figure 5.2	Schematic of a spherical shell and a small square segment of size (a) considered for stability analysis. Boundary of shell segment is assumed to be pin connected with rest of the shell.	23
Figure 5.3	Top view of shell in deformed shape after buckling.	23

Figure 5.4	2D cross section of the locally buckled shell structure.	24
Figure 5.5	Stability curve corresponding to snap through of shell segment.	24
Figure 5.6	Schematic of a spherical shell and a small circular segment of size $(2c)$ of the shell considered for axisymmetric buckling analysis. Boundary of shell segment is assumed to be clamped with rest of the shell.	26
Figure 5.7	Schematic shows cross-section of shell of radius (R) and circular segment of size $(2c)$ before and after buckling of shell. Segment is assumed to be clamped with rest of the shell. Polar coordinate system (r, φ) with origin coinciding with centre of dent formed.	26
Figure 5.8	Variation of stress $\bar{\sigma}_\zeta$ with respect to ζ for various values of k . The total energy of the system extremized with respect to variable ζ and corresponding stresses are named as $\bar{\sigma}_\zeta$. $\bar{\sigma}_\zeta$ plotted for various values of k by varying the dimensionless amplitude ζ .	33
Figure 5.9	Variation of stress $\bar{\sigma}_k$ with respect to ζ for various values of k . The total energy of the system extremized with respect to variable k and corresponding stresses are named as $\bar{\sigma}_\zeta$. $\bar{\sigma}_\zeta$ plotted for various values of k by varying the dimensionless amplitude ζ .	34
Figure 5.10	Variation of stress $\bar{\sigma}_\zeta$ and $\bar{\sigma}_k$ with respect to ζ for various values of k . The total energy of the system extremized with respect to variable ζ and k and corresponding stresses are named as $\bar{\sigma}_\zeta$ and $\bar{\sigma}_k$ respectively. $\bar{\sigma}_\zeta$ and $\bar{\sigma}_k$ plotted for various values of k by varying the dimensionless amplitude ζ .	34
Figure 5.11	Variation of σ with respect to amplitude ζ of displacement w . Resulting curve is locus of points of intersection of curves of σ after minimization of energy with respect to amplitude ζ of	35

displacement w and k . Minimum stress obtained from curve is termed as critical buckling stress.

Figure 5.12	Shell in deformed shape post buckling.	36
Figure 5.13	Top view of shell in deformed shape post buckling.	36
Figure 5.14	2D cross section of the locally buckled shell structure	37
Figure 6.1	Experimental setup showing relative arrangement of different equipment for performing droplet drying experiments.	41
Figure 6.2	Sessile droplet at different stages of drying.	42
Figure 7.1	Variation of critical pressure (p_c) in respect of droplet size for various colloid particle size. Droplet size and particle size are in same unit of measurement.	45
Figure 7.2	Variation of critical pressure (p_c) in respect of colloid particle size for various droplet size. Solid lines are corresponding to upper critical buckling pressure and dashed lines are corresponding to lower critical buckling pressure. Droplet size and particle size are in same unit of measurement.	46
Figure 7.3	Top view of dried granules comprising silica particles with diameters of 1 μm , 3 μm , and 5 μm and with different droplet of volume ranging from 0.5 μL to 5 μL [15].	47
Figure 7.4	Comparison between model prediction and experimental results for dried granules comprising silica particles with diameters of 1 μm , 3 μm , and 5 μm and with different droplet of volume ranging from 0.5 μL to 5 μL as mentioned in Figure 7.3. Here experimental data is represented for various droplet radius corresponding to initial volume mentioned in Figure 7.3.	48

LIST OF TABLES

Table 7.1	Comparison of critical parameters evaluated from two different	43
Table 7.2	Parameter of colloidal droplet of water and silica particles sample	44

NOMENCLATURE

D	Flexural modulus is defined as $D = E_0 h^3 / (1 - \nu^2)$
E_0	Equivalent Young's modulus of shell formed from colloidal droplet during evaporation
f	Amplitude of deflection w
G_p	Shear modulus of particle in packing
h	Thickness of the shell
N	Coordination number of a particle in packing
N_{xx}	Stress resultant in x direction acting on middle surface of shell
N_{xy}	Stress resultant in xy plane acting on middle surface of shell
N_{yy}	Stress resultant in y direction acting on middle surface of shell
M_{xx}	Stress couple due stress in x direction
M_{xy}	Stress couple due stress in xy plane
M_{yy}	Stress couple due stress in y direction
Q_x	Transverse stress resultant in xz plane acting on middle surface of shell
Q_y	Transverse stress resultant in yz plane acting on middle surface of shell
r	Radius of circular segment, polar coordinate in radial direction
R_0	Initial radius of droplet
u	Radial displacement of circular segment
U_b	Strain energy of middle surface due to bending load
U_m	Strain energy of middle surface due membrane forces
w	Deflection of middle surface in z direction
$\nabla^2(\dots)$	Laplace operator

$\nabla_k^2(\dots)$	Vlasov's operator
γ	Surface tension of air-liquid interface
ϵ_0	Strain in shell before onset of buckling
ϵ_{xx}	Normal Strain in x direction
γ_{xy}	Shear Strain in xy plane
ϵ_{yy}	Normal Strain in y direction
χ_x	Change in curvature of middle surface
χ_y	Change in curvature of middle surface
χ_{xy}	Twist of middle surface
ϵ_{rr}	Normal Strain in r direction
$\epsilon_{r\varphi}$	Shear Strain in $r\varphi$ plane
$\epsilon_{\varphi\varphi}$	Normal Strain in φ direction
ν_p	Poisson's ratio of particle in packing
Π	Total potential energy
ϕ	Stress function
φ	Polar coordinate in circumferential direction
ϕ_{rcp}	Random close packing volume fraction at the onset of buckling

Introduction

1.1 Overview

Drying of colloidal droplet occurs in many industrial processes such as spray drying, where the goal is to achieve dried granules of required morphology and density. The study of drying colloidal droplet is very important for fundamental and technological reasons as well. It helps in understanding and mimicking the process occurs in nature for example drying of peas, berry etc. also it helps in understanding drying process in spray drying [1] application at industry level, which is extensively used in food processing industries, pharmaceutical industries, ceramic industries. Colloidal solution or colloid is a stable suspension which is a mixture of nano/micro sized insoluble particles dispersed homogeneously throughout a solvent of another substance. Droplet of colloidal solution of nano/micro sized particles exhibits various morphologies ranging from perfect solid/hollow sphere to toroid along with crumpled surface [2]. The morphology, porosity and mechanical behaviour of final granules govern by number of factors like nano/micro particles size, their volume fraction, droplet size [3], environmental conditions (drying temperature, humidity,) etc.

1.2 Buckling of Colloidal Shell

Buckling instability refers to the phenomenon where a thin shell formed from drying of colloidal droplet loose stability and undergoes deformation, resulting in the formation of irregular shapes or patterns on its surface. Buckling of thin-walled structures is a common occurrence that is critical to a variety of natural processes and industrial applications. When a compressive load acts on the shell, shell loose its flexural load taking capacity and buckling instability occurs. Major cause behind the initiation

of instability in colloidal shell is found to be capillary pressure. Capillary pressure induces due to development of curvature menisci between the contacting colloid particles.

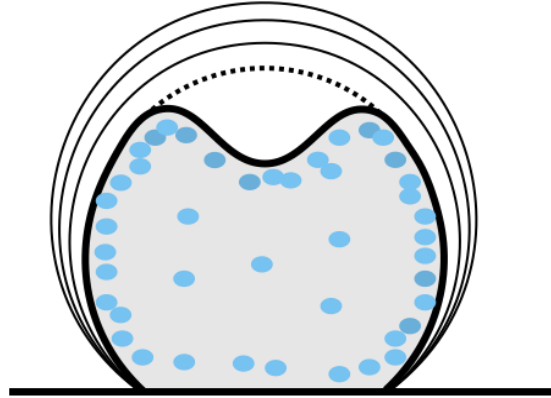


Figure 1.1. Sessile droplet of colloidal solution at various stages of evaporation.



Figure 1.2. Snap through buckling of thin-walled table tennis ball.



Figure 1.3. Dried corn kernels and peas.

1.3 Applications

Spray drying has numerous applications in various industries, few of them are mentioned below :

- (a) Food processing industries: Milk powder, Coffee, Bournvita, Tea, and Flavourings, etc.
- (b) Pharmaceutical industry: Hollow particles for delivering drugs to the lungs, while dense or crumpled particles intended for oral capsules.
- (c) Ceramic industries

1.4 Significance and Objective

From a practical standpoint, there is a dire need to gain a deeper understanding of the intricate drying mechanisms involved in spray drying. The precise understanding of the crucial factors leading to the buckling of a drying suspension drop remains unclear. The relationship between the occurrence of buckling and particle mechanical properties, particle size, the arrangement of particles, and droplet size remains elusive. Therefore, further investigations and studies are required to unravel the complexities of the drying process during spray drying. Furthermore, this understanding aids in simulating natural phenomena and activities. The following are the objectives of the present thesis work :

- (a) To relate the critical buckling pressure to the elastic properties of particle packing in the shell.
- (b) To relate the maximum size of dent formed post buckling with colloid particle size.
- (c) To investigate the post buckling behaviour of shell formed during desiccation of colloidal droplet

The present work aims to provide significant contributions to spray drying applications where same process can be used to achieve dried granule of different morphology and porosity for different applications.

1.5 Thesis Outline

Thesis divided into seven chapters. Work content of each chapter is described here in brief to have an overview of content covered in subsequent chapters. Chapter 2 reviews previous research on understanding the drying kinematics and instability of shell formed during drying of colloidal droplet, effect of colloid solution constituent on buckling behaviour. Chapter 3 introduces theory of shallow shells, the theory used to describe the buckling behaviour of colloidal shell. In chapter 4 analytical study is done of thin spherical shell formed during drying of colloidal droplet using theory of shallow shell considering circular and square segment. Chapter 5 is on experimental methods, in which brief overview of various methods to create spherical droplet for study of drying colloidal droplet is given. Overview of experimental setup to create sessile droplet and for performing droplet drying experiments. Chapter 6 is regarding results and discussion, results from different analysis discussed and compared with experimental data from literature. Chapter 7 conclude the outcome of present study and further scope in present study is also mentioned.

Literature Review

The phenomenon of fast drying in droplets of colloidal suspensions has garnered significant attention among researchers due to the fascinating array of different morphologies observed in the resulting dried granules. These morphologies span from perfectly spherical shapes to intriguing buckled forms reminiscent of deflated balloons or doughnuts [6].

Tsapis et al. [4] were the first to propose a conceptual framework to explain the phenomenon of buckling in drying droplets containing charged colloid suspensions. Their observations revealed that as the droplet undergoes drying, the solvent flux towards the droplet's surface induces the formation of a concentrated shell of particles. Despite the repulsive nature of the colloidal interactions, aggregation can still occur when the Darcy pressure, resulting from the flow of solvent, surpasses the net repulsive stress among the colloids. Consequently, a solid viscoelastic shell is formed, which undergoes further buckling as the drying process progresses and the droplet's volume decreases.

Past work has shown that morphology and spatial distribution of colloid particles in a drying droplet can be controlled by varying the Peclet number [1], $Pe = t_{diffusion}/t_{dry}$. Here, $t_{diffusion}$ is time taken by colloid particles to travel a characteristic length (R). Peclet number relates diffusion and evaporation process and decides their relative dominance over one another. When a droplet of colloidal suspension subjected to dry (Figure 2.1), concentration of colloid particles increases near liquid-air interface due receding liquid-air interface, here two possibility arises. First when ($Pe < 1$), particle get enough time to recirculate inside the droplet to maintain uniform concentration throughout the droplet, drying droplet results in

desiccated dense ball of colloid particles as shown in Figure 2.1. Second when ($Pe > 1$), colloid particles do not get enough time to recirculate inside the droplet and accumulate near liquid-air interface, which results in increased concentration of colloid particles at liquid-air interface relative to inside of droplet. Further evaporation of liquid from the interface lead to rearrangement of particles results in formation of close packing of particles and hence formation of a thin shell. From now further removal of liquid through close packing takes place via capillary action, which builds capillary pressure. Capillary pressure found to be main cause of collapse of close packing formed during drying of colloidal droplet.

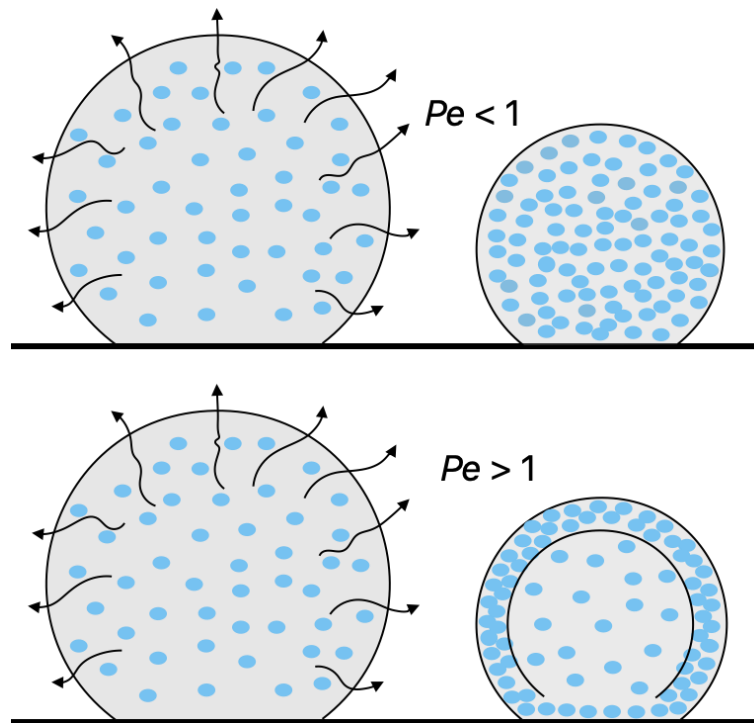


Figure 2.1. Effect of Peclet number on morphology of resultant shell from desiccation of colloidal droplet.

Previous studies presented in Refs. [4] and [9] performed experiment and shown that pressure difference across the shell thickness is in the order of (10^2 - 10^4 Pascal) for particle of sizes ranging from 10 nanometre to 1 micrometre and is characterized by Darcy's law for flow through porous medium. This pressure difference is responsible for radially outward flow

of fluid through the particle packing. The pressure jumps across the liquid–air interface is induced by capillary action is in the order of $(2\gamma/r_p) \sim (10^7 \text{ Pascal})$, where γ is surface tension of liquid and r_p is liquid meniscus radius. It is a result of the curvature of the menisci at the outer layer of particles. Pressure variation across the shell is much smaller as compared to capillary pressure.

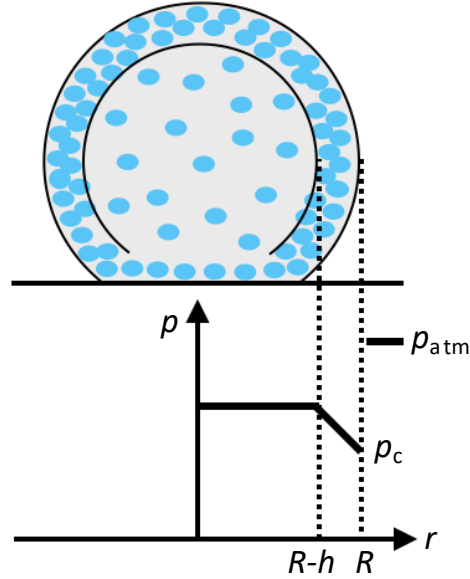


Figure 2.2. Schematic of a sessile droplet drying at a high evaporation rate and the pressure variation in the droplet.

To understand the final morphology and mechanical behaviour of desiccated droplet number of experiments carried out and analogies have been proposed in literature [4]–[7]. Few studies have attempted to address and describe the post buckling behaviour, often assuming a linearly elastic solid for the particle packing and have derived scaling relations for the critical buckling conditions [8]–[10]. In recent study, non-linear elastic parameter derived in terms of particle elastic properties for particle packing and relate to upper critical buckling pressure using small deformation theory of shell [11].

Theory of Shallow Shell for Colloidal Droplet

Theory of thin spherical shell first time was proposed by A. E. H. Love by implying the assumption of thinness. Thin shell theory is based on assumption that one of the three spatial dimension is small as compared to other two. Based on above simplification it is implied that transverse normal to the middle surface remains straight and normal to the middle surface and undergoes no change in length during deformation. The second assumption considered is that transverse normal stress is small in comparison to other normal stresses and may be neglected. The above assumption leads to simplifications of the material constitutive relation through plane stress state in the tangent plane, now then middle surface of the geometry is adequate to consider the deformation analysis. All stresses, strains and elastic energy are defined about the middle surface deformation. In addition to above assumptions basic assumptions like material homogeneity and isotropy remains applicable.

3.1. Governing Differential Equations of Shell Theory

To get started, differential equations that regulate the stresses and strains of elastic spherical shells are derived first, assuming perfectly uniform shells, with no imperfection. Theory of shallow shell is employed for theoretical analysis, where a segment of the shell small enough that slopes relative to a tangent plane at the middle surface point are modest is considered. Then, on this tangent plane, a cartesian coordinate system (x, y) established and shell deformations characterized in terms of tangential displacement fields u, v , and normal deflection w .

The strain-displacement, curvature, and twist-displacement relationship of middle surface in terms of middle surface displacements and deflections u, v and w respectively, are expressed as [12] :

$$\varepsilon_{xx} = \frac{\partial u}{\partial x} - \frac{w}{R_x} + \frac{1}{2} \left(\frac{\partial w}{\partial x} \right)^2 \quad (1a)$$

$$\varepsilon_{yy} = \frac{\partial v}{\partial y} - \frac{w}{R_y} + \frac{1}{2} \left(\frac{\partial w}{\partial y} \right)^2 \quad (1b)$$

$$\gamma_{xy} = \frac{\partial v}{\partial x} + \frac{\partial u}{\partial y} + \frac{\partial w}{\partial x} \frac{\partial w}{\partial y} \quad (1c)$$

$$\chi_x = -\frac{\partial^2 w}{\partial x^2} \quad (1d)$$

$$\chi_y = -\frac{\partial^2 w}{\partial y^2} \quad (1e)$$

$$\chi_{xy} = -\frac{\partial^2 w}{\partial x \partial y} \quad (1f)$$

Stress resultants and stress couples in terms of stress function ϕ and middle surface deflection w , are expressed as:

$$N_{xx} = \frac{\partial^2 \phi}{\partial y^2} \quad (2a)$$

$$N_{yy} = \frac{\partial^2 \phi}{\partial x^2} \quad (2b)$$

$$N_{xy} = N_{yx} = -\frac{\partial^2 \phi}{\partial x \partial y} \quad (2c)$$

$$M_x = -D \left(\frac{\partial^2 w}{\partial x^2} + \nu \frac{\partial^2 w}{\partial y^2} \right) \quad (3a)$$

$$M_y = -D \left(\nu \frac{\partial^2 w}{\partial x^2} + \frac{\partial^2 w}{\partial y^2} \right) \quad (3b)$$

$$M_{xy} = M_{yx} = -D(1 - \nu) \frac{\partial^2 w}{\partial x \partial y} \quad (3c)$$

$$Q_x = -D \frac{\partial(\nabla^2 w)}{\partial x} \quad (4a)$$

$$Q_y = -D \frac{\partial(\nabla^2 w)}{\partial y} \quad (4b)$$

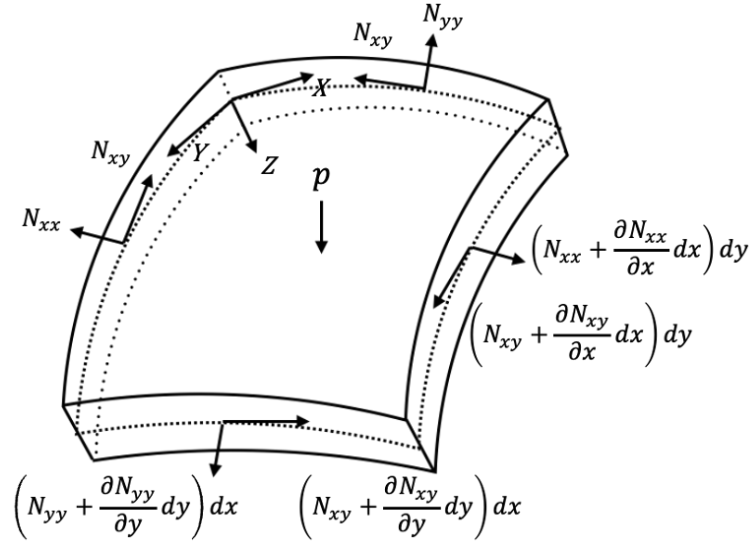


Figure 3.1. The schematic shows the stress resultant and their direction acting on small element characterizing state of stress of the shell element. Note that all stress resultants and stress couples are acting at middle surface of the shell. Z direction is towards the centre of curvature of the shell.

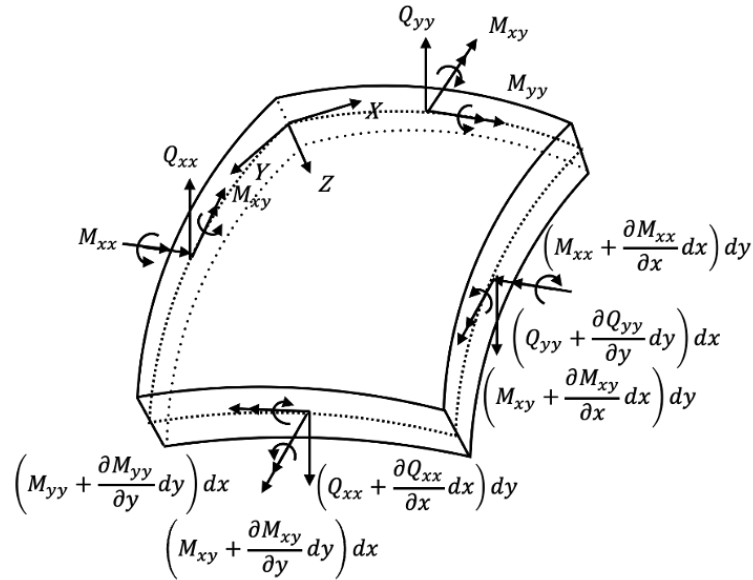


Figure 3.2. The schematic shows the stress resultant and stress couple and their direction acting on small element characterizing state of stress of the shell element. Note that all stress resultants and stress couples are acting at middle surface of the shell. Z direction is towards the centre of curvature of the shell.

The static equilibrium of a small element of shallow shell (Figure 3.1 and Figure 3.2) subjected to a transverse surface load p is described by differential equations expressed as [12] :

$$\frac{\partial N_{xx}}{\partial x} + \frac{\partial N_{xy}}{\partial y} = 0 \quad (5a)$$

$$\frac{\partial N_{yy}}{\partial y} + \frac{\partial N_{xy}}{\partial x} = 0 \quad (5b)$$

$$\frac{\partial Q_x}{\partial x} + \frac{\partial Q_y}{\partial y} + \frac{N_{xx}}{R_x} + \frac{N_{yy}}{R_y} + N_{xx} \frac{\partial^2 w}{\partial x^2} + N_{yy} \frac{\partial^2 w}{\partial y^2} + 2N_{xy} \frac{\partial^2 w}{\partial x \partial y} + p = 0 \quad (5c)$$

$$\frac{\partial M_x}{\partial x} + \frac{\partial M_{xy}}{\partial y} - Q_x = 0 \quad (6a)$$

$$\frac{\partial M_y}{\partial y} + \frac{\partial M_{xy}}{\partial x} - Q_y = 0 \quad (6b)$$

Equations (5) derived by balance of linear momentum, and (6) derived by balance of angular momentum on differential element. Eqs. (5a) and (5b) are identically satisfied, it can be proved by substituting stress resultants from Eq. (2). Substituting the transverse shear forces from Eqs. (6a) and (6b) in Eq. (5c).

$$\begin{aligned} & \frac{\partial^2 M_x}{\partial x^2} + 2 \frac{\partial^2 M_{xy}}{\partial x \partial y} + \frac{\partial^2 M_y}{\partial y^2} + N_{xx} \left(\frac{1}{R_x} + \frac{\partial^2 w}{\partial x^2} \right) + N_{yy} \left(\frac{1}{R_y} + \frac{\partial^2 w}{\partial y^2} \right) + \\ & 2N_{xy} \frac{\partial^2 w}{\partial x \partial y} + p = 0 \end{aligned} \quad (7)$$

Substituting stress resultant and moment, the above Eq. takes the form

$$\frac{D}{h} \nabla^4 w - L(w, \phi) - \frac{1}{R} \nabla^2 \phi - \frac{p}{h} = 0 \quad (8)$$

where Laplace operator is defined as

$$\nabla^2(\dots) = \frac{\partial^2(\dots)}{\partial x^2} + \frac{\partial^2(\dots)}{\partial y^2}, \nabla^4(\dots) = \nabla^2(\nabla^2(\dots)) \quad (9)$$

L is a second order non-linear differential operator in the Eq. (8) is defined as

$$L(f_1, f_2) = \frac{\partial^2 f_1}{\partial y^2} \frac{\partial^2 f_2}{\partial x^2} + \frac{\partial^2 f_1}{\partial x^2} \frac{\partial^2 f_2}{\partial y^2} - 2 \frac{\partial^2 f_1}{\partial x \partial y} \frac{\partial^2 f_2}{\partial x \partial y} \quad (10)$$

Stress resultants in terms of strains are expressed as

$$N_{xx} = \frac{E_0 h}{1-\nu^2} (\varepsilon_x + \nu \varepsilon_y) = \frac{E_0 h}{1-\nu^2} \left(\frac{\partial u}{\partial x} - \frac{w}{R_x} + \frac{1}{2} \left(\frac{\partial w}{\partial x} \right)^2 + \nu \frac{\partial v}{\partial y} - \nu \frac{w}{R_y} + \frac{1}{2} \nu \left(\frac{\partial w}{\partial y} \right)^2 \right) \quad (11)$$

$$N_{yy} = \frac{E_0 h}{1-\nu^2} (\nu \varepsilon_x + \varepsilon_y) = \frac{E_0 h}{1-\nu^2} \left(\nu \frac{\partial u}{\partial x} - \nu \frac{w}{R_x} + \frac{1}{2} \nu \left(\frac{\partial w}{\partial x} \right)^2 + \frac{\partial v}{\partial y} - \frac{w}{R_y} + \frac{1}{2} \left(\frac{\partial w}{\partial y} \right)^2 \right) \quad (12)$$

$$N_{xy} = N_{yx} = \frac{E_0 h}{2(1+\nu)} \left(\frac{\partial v}{\partial x} + \frac{\partial u}{\partial y} + \frac{\partial w}{\partial x} \frac{\partial w}{\partial y} \right) \quad (13)$$

Now eliminating u and v from Eqs. (11), (12) and (13) and evaluating equation of compatibility

$$N_{xx} - \nu N_{yy} = E_0 h \left(\frac{\partial u}{\partial x} - \frac{w}{R_x} + \frac{1}{2} \left(\frac{\partial w}{\partial x} \right)^2 \right) \quad (14)$$

$$N_{yy} - \nu N_{xx} = E_0 h \left(\frac{\partial v}{\partial y} - \frac{w}{R_y} + \frac{1}{2} \left(\frac{\partial w}{\partial y} \right)^2 \right) \quad (15)$$

Using Eqs. (13), (14) and (15)

$$\begin{aligned} & \frac{\partial^2}{\partial y^2} (N_{xx} - \nu N_{yy}) + \frac{\partial^2}{\partial x^2} (N_{yy} - \nu N_{xx}) - 2(1+\nu) \frac{\partial^2 N_{xy}}{\partial x \partial y} \\ &= E_0 h \left\{ \frac{\partial^2}{\partial y^2} \left[\frac{1}{2} \left(\frac{\partial w}{\partial x} \right)^2 \right] + \frac{\partial^2}{\partial x^2} \left[\frac{1}{2} \left(\frac{\partial w}{\partial y} \right)^2 \right] - \frac{\partial^2}{\partial x \partial y} \left(\frac{\partial w}{\partial x} \frac{\partial w}{\partial y} \right) \right\} - \\ & E_0 h \left\{ \frac{1}{R_x} \frac{\partial^2 w}{\partial y^2} + \frac{1}{R_y} \frac{\partial^2 w}{\partial x^2} \right\} \end{aligned} \quad (16)$$

$$\begin{aligned} & \frac{\partial^2}{\partial y^2} (N_{xx} - \nu N_{yy}) + \frac{\partial^2}{\partial x^2} (N_{yy} - \nu N_{xx}) - 2(1+\nu) \frac{\partial^2 N_{xy}}{\partial x \partial y} \\ &= E_0 h \left\{ \left(\frac{\partial^2 w}{\partial x \partial y} \right)^2 - \frac{\partial^2 w}{\partial x^2} \frac{\partial^2 w}{\partial y^2} - \frac{1}{R_x} \frac{\partial^2 w}{\partial y^2} - \frac{1}{R_y} \frac{\partial^2 w}{\partial x^2} \right\} \end{aligned} \quad (17)$$

Substituting stress resultants in Eq. (17) using Eq. (2) in terms of stress functions, Eq. (17) takes the form

$$\nabla^2 \nabla^2 \phi = E_0 h \left\{ \left(\frac{\partial^2 w}{\partial x \partial y} \right)^2 - \frac{\partial^2 w}{\partial x^2} \frac{\partial^2 w}{\partial y^2} - \frac{1}{R_x} \frac{\partial^2 w}{\partial y^2} - \frac{1}{R_y} \frac{\partial^2 w}{\partial x^2} \right\} \quad (18)$$

For spherical shell $R_x = R_y$. Rewriting the above Eq. in the following form

$$\frac{1}{E_0} \nabla^2 \nabla^2 \phi + \frac{1}{2} L(w, w) + \frac{1}{R} \nabla^2 w = 0 \quad (19)$$

Equation (19) is equation of compatibility, where Laplace operator and L operator are defined in Eqs. (09) and (10). Stability of thin shell formed during drying of colloidal droplet is governed by fourth order differential Eqs. (08) and (19) together in terms of mid-plane deflection w and stress function ϕ . Direct solution of these shallow shell equations is quite difficult and challenging due to the presence of nonlinear operator but using approximate techniques they can be solved with required level of accuracy.

3.2. Parameters in Polar Coordinates

Analysing the circular geometry, it is preferable to use polar coordinate system (r, φ) instead of cartesian coordinate (x, y) , with origin coinciding with centre of circular segment. Strain, curvature, and twist in polar coordinate are expressed as

$$\varepsilon_{rr} = \frac{\partial u}{\partial r} - \frac{w}{R} + \frac{1}{2} \left(\frac{\partial w}{\partial r} \right)^2 \quad (20a)$$

$$\varepsilon_{\varphi\varphi} = \frac{u}{R} + \frac{1}{r} \frac{\partial v}{\partial \varphi} - \frac{w}{R} + \frac{1}{2} \left(\frac{1}{r} \frac{\partial w}{\partial \varphi} \right)^2 \quad (20b)$$

$$\gamma_{r\varphi} = \left(\frac{1}{r} \frac{\partial u}{\partial \varphi} + \frac{\partial v}{\partial r} - \frac{v}{r} + \frac{1}{r} \frac{\partial w}{\partial r} \frac{\partial w}{\partial \varphi} \right) \quad (20c)$$

$$\chi_{rr} = \frac{\partial^2 w}{\partial r^2} \quad (20d)$$

$$\chi_{\varphi\varphi} = \frac{1}{r} \frac{\partial w}{\partial r} + \frac{1}{r^2} \frac{\partial^2 w}{\partial r^2} \quad (20e)$$

$$\chi_{r\varphi} = \frac{1}{r} \frac{\partial^2 w}{\partial r \partial \varphi} - \frac{1}{r^2} \frac{\partial w}{\partial \varphi} \quad (20f)$$

Stress in terms of stress function ϕ are expressed as

$$\sigma_{rr} = \frac{1}{r} \frac{\partial \phi}{\partial r} + \frac{1}{r^2} \frac{\partial^2 \phi}{\partial \varphi^2}, \quad \sigma_{\varphi\varphi} = \frac{\partial^2 \phi}{\partial r^2}, \quad \tau_{r\varphi} = \frac{1}{r^2} \frac{\partial \phi}{\partial \varphi} - \frac{1}{r} \frac{\partial^2 \phi}{\partial r \partial \varphi} \quad (21)$$

Stresses in terms of stress function ϕ for axisymmetric case are expressed as

$$\sigma_{rr} = \frac{1}{r} \frac{d\phi}{dr}, \quad \sigma_{\phi\phi} = \frac{d^2\phi}{dr^2}, \quad \tau_{r\phi} = 0 \quad (22)$$

Governing differential equations remains same for polar coordinate but L and ∇ operator for axisymmetric case in polar coordinate are expressed as

$$L(w, \phi) = \frac{1}{r} \left(\frac{d^2w}{dr^2} \frac{d\phi}{dr} + \frac{dw}{dr} \frac{d^2\phi}{dr^2} \right) \quad (23a)$$

$$L(w, w) = \frac{2}{r} \left(\frac{d^2w}{dr^2} \frac{dw}{dr} \right) \quad (23b)$$

$$\nabla^2(\dots) = \frac{\partial^2(\dots)}{\partial r^2} + \frac{1}{r} \frac{\partial(\dots)}{\partial r} + \frac{1}{r^2} \frac{\partial^2(\dots)}{\partial \phi^2}, \quad \nabla^4(\dots) = \nabla^2(\nabla^2(\dots)) \quad (24)$$

For axisymmetric case

$$\nabla^2 = \frac{1}{r} \frac{d}{dr} \left(r \frac{d}{dr} \right) \quad (25)$$

Equivalent Elastic Parameter

Stability analysis of spherical shell is done using equivalent elastic parameter for random close packing in shell. Equivalent elastic parameter for random close packing in shell assumed to be function of colloid particle elastic properties and volume fraction of particles and their coordination number in the packing. Stability analysis is done considering elastic parameter proposed by [3] for spherical shell of randomly close packed particles in terms of colloid particle Young's modulus, Poisson's ratio, and volume fraction of particle in shell.

$$E_0 = \frac{5\pi}{16} \bar{G} \varepsilon_0^{1/2} \quad (26)$$

$$\text{where } \bar{G} = \frac{\phi_{rcp} N G_p}{2\pi(1-\nu_p)} \quad (27)$$

Following assumptions are considered while deriving parameter proposed above:

- (a) Pressure variation across the packing is neglected.
- (b) Pressure variation in the interior of the shell is neglected.
- (c) At the time of cracking or buckling the response of the same can be seen in two different time limits, short time limits and long-time limits. Here, long time limit is considered and hence neglected the capillary pressure variation.

Stability Analysis of Colloidal Droplet

Stability analysis of spherical shell of colloid particles is done using theory of shallow shell. Analysis is done by considering two different segments, for one case square segment is considered assuming segment is pin connected with rest of the shell and for second case circular segment is considered assuming segment is clamped with rest of the shell.

5.1. Stability Analysis of Spherical Shell Considering Square Segment

Stability analysis is performed to describe the behaviour of the shell post buckling. Geometrically non-linear theory of shallow shell is used to describe the buckling behaviour of thin spherical shell forms during drying of colloidal droplet. Shallow shells refer to structures whose rise is small as compared to their span. Since dent forming in the bucking of spherical shell is comparable to shallow shells so nonlinear theory of shallow shell can be applied. To do that a small square segment (of size a) of top surface of the shell is considered (Figure 5.1). Shell edges are assumed to be pin connected with rest of the shell, which is rigid in its own plane and flexible out of the plane for bending. Also, it is assumed that points along the shell are free to slide. Corresponding to these, boundary conditions are expressed as

$$w = 0, \frac{\partial^2 w}{\partial x^2} = 0, \sigma_1 = 0, \tau_{xy} = 0 \quad \text{at } x = \pm a/2 \quad (28a)$$

$$w = 0, \frac{\partial^2 w}{\partial y^2} = 0, \sigma_2 = 0, \tau_{yx} = 0 \quad \text{at } y = \pm a/2 \quad (28b)$$

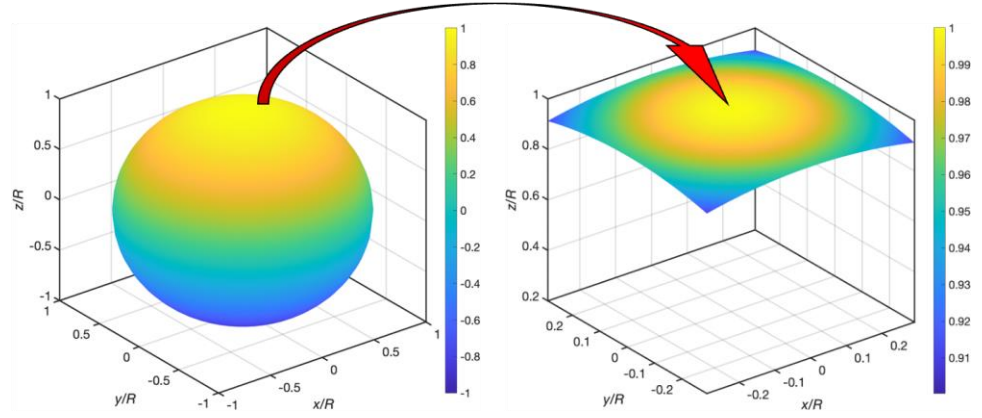


Figure 5.1. Schematic of a spherical shell and a small square segment of size (a) considered for stability analysis. Boundary of shell segment is assumed to be pin connected with rest of the shell.

The Galerkin method which belongs to the variational method to solve the boundary value problem approximately is applied here to study the buckling behaviour of buckled shell in terms of deformation. Here condition of stability will be evaluated by varying size of square segment and maximum deflection of middle surface. The assumed expression for stress function (ϕ) and deflection (w) of middle surface in transverse direction is kept function of coordinate x and y , are expressed as

$$\text{Stress function: } \phi = A \cos\left(\frac{\pi x}{a}\right) \cos\left(\frac{\pi y}{a}\right) \quad (29a)$$

$$\text{Deflection function: } w = B \cos\left(\frac{\pi x}{a}\right) \cos\left(\frac{\pi y}{a}\right) \quad (29b)$$

These functions satisfy first three boundary conditions and fourth boundary condition satisfied in an averaged manner over the length of the edge and method presented by A.S. Volm'ir [13] has been employed for stability analysis of shallow panel and governing equations of nonlinear shallow shell theory. Weighted residual statement for Galerkin method are expressed as

$$\int_{-a/2}^{a/2} \int_{-a/2}^{a/2} X \cos\left(\frac{\pi x}{a}\right) \cos\left(\frac{\pi y}{a}\right) dx dy = 0 \quad (30a)$$

$$\int_{-a/2}^{a/2} \int_{-a/2}^{a/2} Y \cos\left(\frac{\pi x}{a}\right) \cos\left(\frac{\pi y}{a}\right) dx dy = 0 \quad (30b)$$

where X and Y are residues corresponding to differential Eqs. (08) and (19) are expressed as

$$X = \frac{D}{h} \nabla^2 \nabla^2 w - \frac{1}{R} \nabla^2 \phi - L(\phi, w) - \frac{p}{h} \quad (31a)$$

$$Y = \frac{1}{E_0} \nabla^2 \nabla^2 \phi + \frac{1}{2} L(w, w) + \frac{1}{R} \nabla^2 w \quad (31b)$$

Evaluating the derivatives of w and ϕ appearing in the residual statement

$$\nabla^2 w = -\frac{2\pi^2}{a^2} B \cos\left(\frac{\pi x}{a}\right) \cos\left(\frac{\pi y}{a}\right) \quad (32a)$$

$$\nabla^4 w = \frac{4\pi^4}{a^4} B \cos\left(\frac{\pi x}{a}\right) \cos\left(\frac{\pi y}{a}\right) \quad (32b)$$

$$\nabla^2 \phi = -\frac{2\pi^2}{a^2} A \cos\left(\frac{\pi x}{a}\right) \cos\left(\frac{\pi y}{a}\right) \quad (32c)$$

$$\nabla^4 \phi = \frac{4\pi^4}{a^4} A \cos\left(\frac{\pi x}{a}\right) \cos\left(\frac{\pi y}{a}\right) \quad (32d)$$

$$L(\phi, w) = \frac{2\pi^4}{a^4} AB \left[\cos^2\left(\frac{\pi x}{a}\right) \cos^2\left(\frac{\pi y}{a}\right) - \sin^2\left(\frac{\pi x}{a}\right) \sin^2\left(\frac{\pi y}{a}\right) \right] \quad (32e)$$

$$L(w, w) = \frac{2\pi^4}{a^4} B^2 \left[\sin^2\left(\frac{\pi x}{a}\right) \sin^2\left(\frac{\pi y}{a}\right) - \sin^2\left(\frac{\pi x}{a}\right) \sin^2\left(\frac{\pi y}{a}\right) \right] \quad (32f)$$

Now evaluating the first residual statement, Eq. (30a)

$$\int_{-a/2}^{a/2} \int_{-a/2}^{a/2} \left[\frac{D}{h} \nabla^2 \nabla^2 w - \frac{1}{R} \nabla^2 \phi - L(\phi, w) - \frac{p}{h} \right] \cos\left(\frac{\pi x}{a}\right) \cos\left(\frac{\pi y}{a}\right) dx dy = 0 \quad (33)$$

Evaluating all component by substituting w and ϕ and their derivatives and integrating over the domain

1st term

$$\begin{aligned} & \int_{-a/2}^{a/2} \int_{-a/2}^{a/2} \left[\frac{D}{h} \nabla^2 \nabla^2 w \right] \cos\left(\frac{\pi x}{a}\right) \cos\left(\frac{\pi y}{a}\right) dx dy \\ &= \int_{-a/2}^{a/2} \int_{-a/2}^{a/2} \left[\frac{D}{h} \frac{4\pi^4}{a^4} B \cos\left(\frac{\pi x}{a}\right) \cos\left(\frac{\pi y}{a}\right) \right] \cos\left(\frac{\pi x}{a}\right) \cos\left(\frac{\pi y}{a}\right) dx dy \end{aligned}$$

$$\begin{aligned}
&= \frac{D}{h} \frac{4\pi^4}{a^4} B \left(\frac{a^2}{4} \right) \\
&= \frac{D}{h} \frac{\pi^4}{a^2} B
\end{aligned} \tag{34a}$$

2nd term

$$\begin{aligned}
&\int_{-a/2}^{a/2} \int_{-a/2}^{a/2} \left[\frac{1}{R} \nabla^2 \phi \right] \cos \left(\frac{\pi x}{a} \right) \cos \left(\frac{\pi y}{a} \right) dx dy \\
&= \int_{-a/2}^{a/2} \int_{-a/2}^{a/2} \left[-\frac{1}{R} \frac{2\pi^2}{a^2} A \cos \left(\frac{\pi x}{a} \right) \cos \left(\frac{\pi y}{a} \right) \right] \cos \left(\frac{\pi x}{a} \right) \cos \left(\frac{\pi y}{a} \right) dx dy \\
&= -\frac{1}{R} \frac{2\pi^2}{a^2} \left(\frac{a^2}{4} \right) \\
&= -\frac{\pi^2 A}{2 R}
\end{aligned} \tag{34b}$$

3rd term

$$\begin{aligned}
&\int_{-a/2}^{a/2} \int_{-a/2}^{a/2} [L(\phi, w)] \cos \left(\frac{\pi x}{a} \right) \cos \left(\frac{\pi y}{a} \right) dx dy \\
&= \int_{-a/2}^{a/2} \int_{-a/2}^{a/2} \frac{2\pi^4}{a^4} AB \left[\cos^2 \left(\frac{\pi x}{a} \right) \cos^2 \left(\frac{\pi y}{a} \right) - \right. \\
&\quad \left. \sin^2 \left(\frac{\pi x}{a} \right) \sin^2 \left(\frac{\pi y}{a} \right) \right] \cos \left(\frac{\pi x}{a} \right) \cos \left(\frac{\pi y}{a} \right) dx dy \\
&= \int_{-a/2}^{a/2} \int_{-a/2}^{a/2} \frac{2\pi^4}{a^4} AB \left[\cos^3 \left(\frac{\pi x}{a} \right) \cos^3 \left(\frac{\pi y}{a} \right) - \right. \\
&\quad \left. \sin^2 \left(\frac{\pi x}{a} \right) \sin^2 \left(\frac{\pi y}{a} \right) \cos \left(\frac{\pi x}{a} \right) \cos \left(\frac{\pi y}{a} \right) \right] dx dy \\
&= \frac{2\pi^4}{a^4} AB \left(\frac{16a^2}{9\pi^2} - \frac{4a^2}{9\pi^2} \right) \\
&= \frac{8}{3} \frac{\pi^2}{a^2} AB
\end{aligned} \tag{34c}$$

4th term

$$\int_{-a/2}^{a/2} \int_{-a/2}^{a/2} \left[\frac{p}{h} \right] \cos \left(\frac{\pi x}{a} \right) \cos \left(\frac{\pi y}{a} \right) dx dy = \frac{p}{h} \left(\frac{4a^2}{\pi^2} \right) \tag{34d}$$

Substituting all integration component in Eq. (33)

$$\frac{D}{h} \frac{\pi^4}{a^2} B + \frac{\pi^2 A}{2 R} - \frac{8}{3} \frac{\pi^2}{a^2} AB - \frac{p}{h} \frac{4a^2}{\pi^2} = 0$$

$$\frac{D}{h} \frac{\pi^4}{4a^2} B + \frac{\pi^2 A}{8R} - \frac{2\pi^2}{3a^2} AB - \frac{p a^2}{h \pi^2} = 0$$

$$A = \left[\frac{p 4a^2}{h \pi^2} - \frac{D}{h} \frac{\pi^4}{4a^2} B \right] / \left[\frac{\pi^2}{8R} - \frac{2\pi^2}{3a^2} B \right] \quad (35)$$

Now solving second residual statement, Eq. (31b)

$$\int_{-a/2}^{a/2} \int_{-a/2}^{a/2} \left[\frac{1}{E_0} \nabla^2 \nabla^2 \phi + \frac{1}{2} L(w, w) + \frac{1}{R} \nabla^2 w \right] \cos\left(\frac{\pi x}{a}\right) \cos\left(\frac{\pi y}{a}\right) dx dy = 0 \quad (36)$$

1st rem

$$\begin{aligned} & \int_{-a/2}^{a/2} \int_{-a/2}^{a/2} \left[\frac{1}{E_0} \nabla^2 \nabla^2 \phi \right] \cos\left(\frac{\pi x}{a}\right) \cos\left(\frac{\pi y}{a}\right) dx dy \\ &= \int_{-a/2}^{a/2} \int_{-a/2}^{a/2} \left[\frac{1}{E_0} \frac{4\pi^4}{a^4} A \cos\left(\frac{\pi x}{a}\right) \cos\left(\frac{\pi y}{a}\right) \right] \cos\left(\frac{\pi x}{a}\right) \cos\left(\frac{\pi y}{a}\right) dx dy \\ &= \frac{1}{E_0} \frac{4\pi^4}{a^4} A \left(\frac{a^2}{4} \right) \\ &= \frac{\pi^4}{a^2} \frac{A}{E_0} \end{aligned} \quad (37a)$$

2nd term

$$\begin{aligned} & \int_{-a/2}^{a/2} \int_{-a/2}^{a/2} \left[\frac{1}{2} L(w, w) \right] \cos\left(\frac{\pi x}{a}\right) \cos\left(\frac{\pi y}{a}\right) dx dy \\ &= \int_{-a/2}^{a/2} \int_{-a/2}^{a/2} \frac{2\pi^4}{a^4} B^2 \left[\cos^2\left(\frac{\pi x}{a}\right) \cos^2\left(\frac{\pi y}{a}\right) - \sin^2\left(\frac{\pi x}{a}\right) \sin^2\left(\frac{\pi y}{a}\right) \right] \cos\left(\frac{\pi x}{a}\right) \cos\left(\frac{\pi y}{a}\right) dx dy \\ &= \int_{-a/2}^{a/2} \int_{-a/2}^{a/2} \frac{2\pi^4}{a^4} B^2 \left[\cos^3\left(\frac{\pi x}{a}\right) \cos^3\left(\frac{\pi y}{a}\right) - \sin^2\left(\frac{\pi x}{a}\right) \sin^2\left(\frac{\pi y}{a}\right) \cos\left(\frac{\pi x}{a}\right) \cos\left(\frac{\pi y}{a}\right) \right] dx dy \\ &= \frac{\pi^4}{a^4} B^2 \left[\frac{16a^2}{9\pi^2} - \frac{4a^2}{9\pi^2} \right] \\ &= \frac{4}{3} \frac{\pi^2}{a^2} B^2 \end{aligned} \quad (37b)$$

3rd term

$$\begin{aligned}
& \int_{-a/2}^{a/2} \int_{-a/2}^{a/2} \left[\frac{1}{R} \nabla^2 w \right] \cos\left(\frac{\pi x}{a}\right) \cos\left(\frac{\pi y}{a}\right) dx dy \\
&= \int_{-a/2}^{a/2} \int_{-a/2}^{a/2} \left[-\frac{1}{R} \frac{2\pi^2}{a^2} B \cos\left(\frac{\pi x}{a}\right) \cos\left(\frac{\pi y}{a}\right) \right] \cos\left(\frac{\pi x}{a}\right) \cos\left(\frac{\pi y}{a}\right) dx dy \\
&= -\frac{1}{R} \frac{\pi^2}{2} B - \frac{1}{R} \frac{2\pi^2}{a^2} B \frac{a^2}{4} \tag{37c}
\end{aligned}$$

Now, substituting all integration component in Eq. (36)

$$\frac{\pi^4}{a^2} \frac{A}{E_0} + \frac{4}{3} \frac{\pi^2}{a^2} B^2 - \frac{1}{R} \frac{\pi^2}{2} B = 0 \tag{38}$$

Substituting A from (35) in above Eq.

$$\begin{aligned}
& \frac{\pi^4}{a^2} \frac{A}{E_0} \left[\frac{p}{h} \frac{4a^2}{\pi^2} - \frac{D}{h} \frac{\pi^4}{4a^2} B \right] + \frac{4}{3} \frac{\pi^2}{a^2} B^2 \left[\frac{\pi^2}{8} \frac{1}{R} - \frac{2}{3} \frac{\pi^2}{a^2} B \right] - \frac{1}{R} \frac{\pi^2}{2} B \left[\frac{\pi^2}{8} \frac{1}{R} - \right. \\
& \left. \frac{2}{3} \frac{\pi^2}{a^2} B \right] = 0
\end{aligned}$$

$$\begin{aligned}
& \frac{\pi^4}{a^2} \frac{1}{E_0} \frac{p}{h} \frac{4a^2}{\pi^2} - \frac{\pi^4}{a^2} \frac{1}{E_0} \frac{D}{h} \frac{\pi^4}{4a^2} B + \frac{4}{3} \frac{\pi^2}{a^2} B^2 \frac{\pi^2}{8} \frac{1}{R} - \frac{4}{3} \frac{\pi^2}{a^2} B^2 \frac{2}{3} \frac{\pi^2}{a^2} B - \\
& \frac{1}{R} \frac{\pi^2}{2} B \frac{\pi^2}{8} \frac{1}{R} + \frac{1}{R} \frac{\pi^2}{2} B \frac{2}{3} \frac{\pi^2}{a^2} B = 0
\end{aligned}$$

$$4\pi^2 \frac{1}{E_0} \frac{p}{h} - \frac{\pi^8}{4} \frac{DB}{E_0 h a^4} + \frac{\pi^4}{6} \frac{B^2}{R a^2} - \frac{8\pi^4}{9} \frac{B^3}{a^4} - \frac{\pi^4}{16} \frac{B}{R^2} + \frac{\pi^4}{3} \frac{B^2}{R a^2} = 0$$

Multiplying by $R^2/4\pi^2 h$

$$\frac{p}{E_0} \left(\frac{R}{h} \right)^2 - \frac{2\pi^2}{9} \frac{B^3 R^2}{h a^4} + \frac{\pi^2}{24} \frac{B^2 R}{h a^2} + \frac{\pi^2}{12} \frac{B^2 R}{h a^2} - \frac{\pi^2}{64} \frac{B}{h} - \frac{\pi^6}{192(1-\nu^2)} \frac{B R^2 h}{a^4} = 0$$

$$\frac{p}{E_0} \left(\frac{R}{h} \right)^2 - \frac{2\pi^2}{9} \frac{B^3 R^2}{h a^4} + \frac{\pi^2}{8} \frac{B^2 R}{h a^2} - \frac{\pi^2}{64} \frac{B}{h} - \frac{\pi^6}{192(1-\nu^2)} \frac{B R^2 h}{a^4} = 0 \tag{39}$$

Introducing following dimensionless parameter in Eq. (39)

$$k = \frac{a^2}{Rh}; \quad \zeta = \frac{B}{h}; \quad \bar{p} = \frac{p}{E_0} \left(\frac{R}{h} \right)^2$$

Substituting above mentioned dimensionless parameter, Eq. (39) is expressed as

$$\bar{p} = \frac{2\pi^2}{9} \frac{\zeta^3}{k^2} - \frac{\pi^2}{8} \frac{\zeta^2}{k} + \left[\frac{\pi^2}{64} + \frac{\pi^6}{192(1-\nu^2)k^2} \right] \zeta \tag{40}$$

Now evaluating $\frac{d\bar{p}}{d\zeta} = 0$ to get value of ζ corresponding to upper and lower critical buckling pressure

$$\frac{2\pi^2}{3} \frac{\zeta^2}{k^2} - \frac{\pi^2}{4} \frac{\zeta}{k} + \left[\frac{\pi^2}{64} + \frac{\pi^6}{192(1-\nu^2)k^2} \right] = 0$$

Solution of above quadratic equation is

$$\zeta = \frac{\frac{\pi^2}{4k} \pm \sqrt{\left(\frac{\pi^2}{4k}\right)^2 - \frac{8\pi^2}{3k^2} \left[\frac{\pi^2}{64} + \frac{\pi^6}{192(1-\nu^2)k^2}\right]}}{\frac{4\pi^2}{3k^2}} \quad (41)$$

Value of k corresponding to snap through of shell segment, expression under radical sign must be zero

$$\left(\frac{\pi^2}{4k}\right)^2 - \frac{8\pi^2}{3k^2} \left[\frac{\pi^2}{64} + \frac{\pi^6}{192(1-\nu^2)k^2}\right]$$

$$\frac{\pi^4}{16k^2} - \frac{\pi^4}{24k^2} - \frac{\pi^8}{72(1-\nu^2)k^4} = 0$$

$$\frac{\pi^4}{48} - \frac{\pi^8}{72(1-\nu^2)k^2} = 0$$

$$k = \pi^2 \sqrt{\frac{2}{3(1-\nu^2)}} \quad \text{at } \zeta = \frac{3}{16} k \quad (42)$$

For $\nu = 1/3$, $k = 8.5473$ at $\zeta = 1.6026$ and $\bar{p} = 0.1235$. Critical buckling pressure corresponding to these is

$$p = 0.1235E_0 \left(\frac{h}{R}\right)^2 \quad (43)$$

Figures (5.2-5.4) shows the deformed shape of droplet. Stability curve corresponding to condition in Eq. (42) is shown in Figure (5.5).

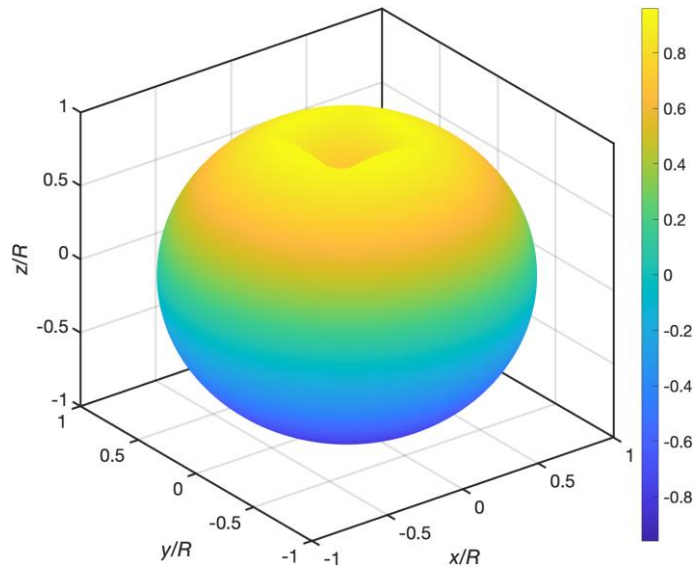


Figure 5.2. Shell in deformed shape after buckling

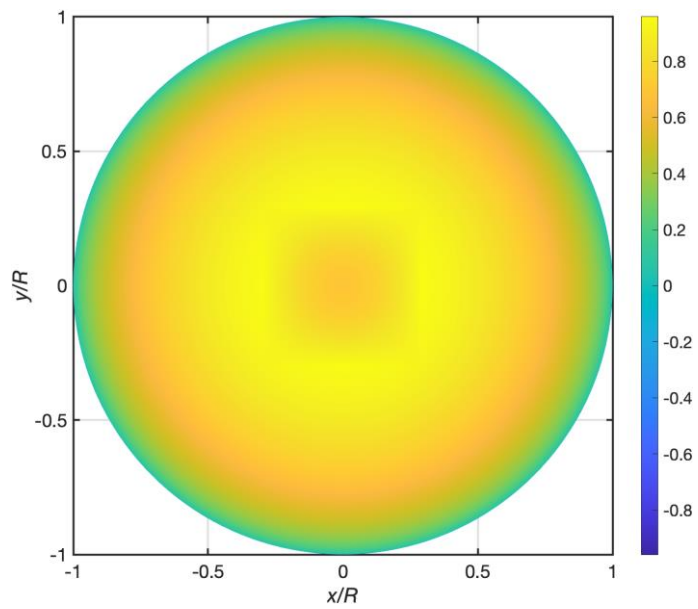


Figure 5.3. Top view of shell in deformed shape after buckling

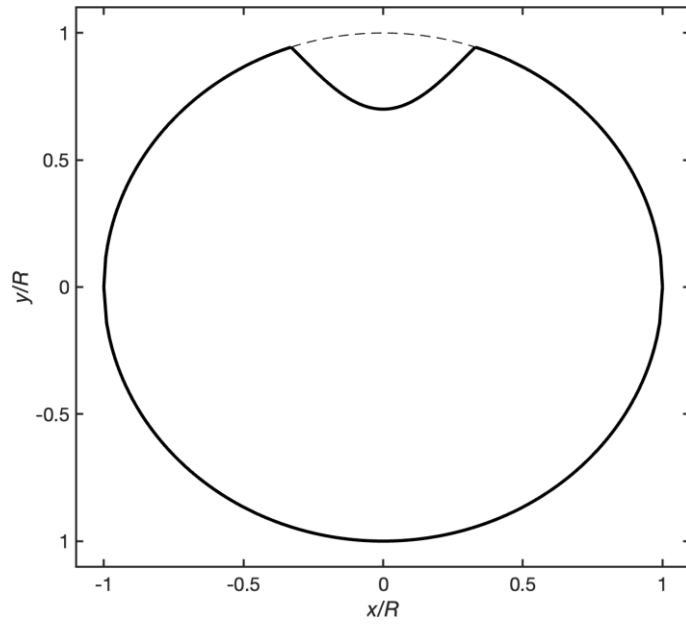


Figure 5.4. 2D cross section of the locally buckled shell structure.

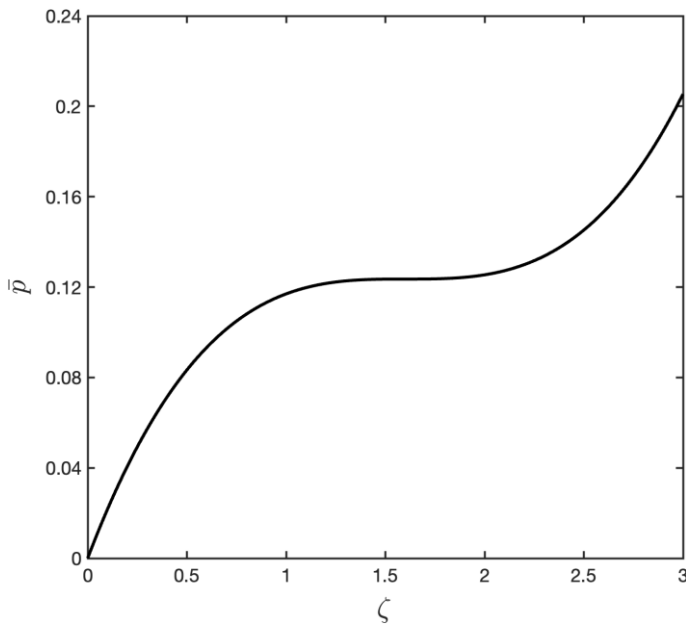


Figure 5.5. Stability curve corresponding to snap through of shell segment.

5.2. Stability Analysis of Spherical Shell Considering Circular Segment

Theoretical analysis is performed considering that shell buckling behaviour is axisymmetric and same is found in experiments performed also. Assuming that boundary conditions, load, geometry, and material properties are axisymmetric. Geometrically non-linear theory of shallow shell is used to describe the buckling behaviour of thin spherical shell forms during drying of colloidal droplet. Shallow shells refer to structures whose rise is small as compared to their span. Since dent forming in the buckling of spherical shell is comparable to shallow shells so nonlinear theory of shallow shell can be applied.

The Ritz method which belongs to the variational method to solve the boundary value problem approximately is applied here to study the buckling behaviour of buckled shell in terms of deformation. The Ritz method applies the principle of minimum potential energy. Here condition of stability will be evaluated by varying size of circular segment and maximum deflection of middle surface (adopted the approach given in [13]). The assumed expression for deflection of middle surface in transverse direction is kept function of radius of dent only for axisymmetric case is expressed as

$$w = f \left(1 - \frac{r^2}{c^2} \right)^2 \quad (44)$$

Now establishing boundary conditions, circular segment considered for the analysis is assumed to be clamped with rest of the shell and there is no movement of boundary edge in the radial direction of circular segment. Above mentioned boundary conditions are expressed as

$$w = 0, \quad \frac{dw}{dr} = 0 \quad \text{at } r = c \quad (45a)$$

$$u = \frac{r}{E_0} \left(\frac{d^2\phi}{dr^2} - \frac{\nu}{r} \frac{d\phi}{dr} \right) = 0 \quad \text{at } r = c \quad (45b)$$

Further, at $r = 0$, radial stress must be bounded to zero

$$\sigma_{rr} = \frac{1}{r} \frac{d\phi}{dr} = 0 \quad (45c)$$

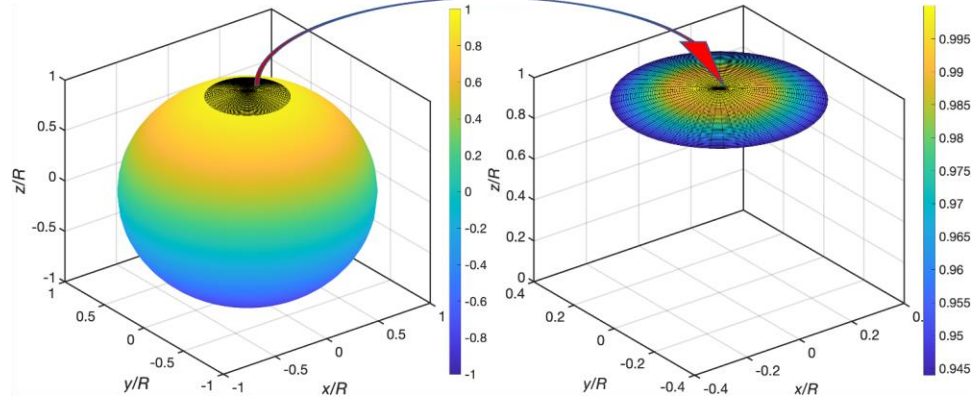


Figure 5.6. Schematic of a spherical shell and a small circular segment of size $(2c)$ of the shell considered for axisymmetric buckling analysis. Boundary of shell segment is assumed to be clamped with rest of the shell.

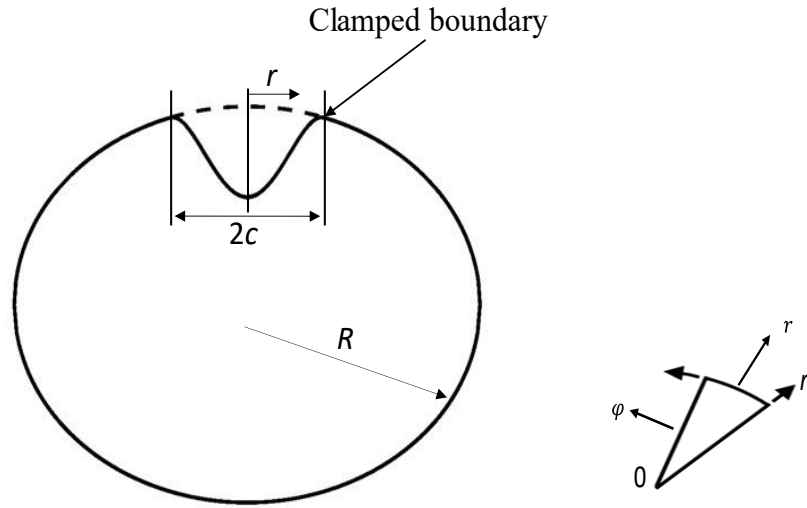


Figure 5.7. Schematic shows cross-section of shell of radius R and circular segment of size $(2c)$ before and after buckling of shell. Segment is assumed to be clamped with rest of the shell. Polar coordinate system (r, φ) with origin coinciding with centre of dent formed.

Stress function ϕ is evaluated from governing equations by applying boundary condition. Now solving the governing differential Eq. (08) in polar coordinate system. Substituting the Eqs. (23) and (25) in Eq. (08) and integrating with respect to r .

$$\frac{D}{h} \frac{1}{r} \frac{d}{dr} \left(r \frac{d(\nabla^2 w)}{dr} \right) = \frac{1}{r} \left(\frac{d^2 w}{dr^2} \frac{d\phi}{dr} + \frac{dw}{dr} \frac{d^2 \phi}{dr^2} \right) + \frac{1}{R} \frac{1}{r} \frac{d}{dr} \left(r \frac{d\phi}{dr} \right) + \frac{p}{h} \quad (46)$$

$$\frac{D}{h} \frac{d}{dr} \left(r \frac{d(\nabla^2 w)}{dr} \right) = \left(\frac{d^2 w}{dr^2} \frac{d\phi}{dr} + \frac{dw}{dr} \frac{d^2 \phi}{dr^2} \right) + \frac{1}{R} \frac{d}{dr} \left(r \frac{d\phi}{dr} \right) + \frac{rp}{h} \quad (47)$$

$$\frac{D}{h} \left(r \frac{d(\nabla^2 w)}{dr} \right) = \left(\frac{d\phi}{dr} \frac{dw}{dr} \right) + \frac{1}{R} \left(r \frac{d\phi}{dr} \right) + \int_0^r \frac{rp}{h} \frac{rp}{h} dr \quad (48)$$

$$\frac{D}{h} \left(\frac{d(\nabla^2 w)}{dr} \right) = \frac{1}{r} \left(\frac{d\phi}{dr} \frac{dw}{dr} \right) + \frac{1}{R} \left(\frac{d\phi}{dr} \right) + \frac{1}{r} \int_0^r \frac{rp}{h} dr \quad (49)$$

Now solving the governing differential Eq. (19) in polar coordinate system. Substituting the Eqs. (23) and (25) in Eq. (19) and integrating with respect to r .

$$\frac{1}{E_0} \frac{1}{r} \frac{d}{dr} \left(r \frac{d(\nabla^2 \phi)}{dr} \right) + \frac{1}{r} \left(\frac{d^2 w}{dr^2} \frac{dw}{dr} \right) + \frac{1}{R} \frac{1}{r} \frac{d}{dr} \left(r \frac{dw}{dr} \right) = 0 \quad (50)$$

$$\frac{1}{E_0} \frac{d}{dr} \left(r \frac{d(\nabla^2 \phi)}{dr} \right) + \left(\frac{d^2 w}{dr^2} \frac{dw}{dr} \right) + \frac{1}{R} \frac{d}{dr} \left(r \frac{dw}{dr} \right) = 0 \quad (51)$$

$$\frac{1}{E_0} \left(r \frac{d(\nabla^2 \phi)}{dr} \right) + \frac{1}{2} \left(\frac{dw}{dr} \right)^2 + \frac{1}{R} \left(r \frac{dw}{dr} \right) = 0 \quad (52)$$

$$\frac{d(\nabla^2 \phi)}{dr} = -E_0 \left[\frac{1}{2r} \left(\frac{dw}{dr} \right)^2 + \frac{1}{R} \left(\frac{dw}{dr} \right) \right] \quad (53)$$

Substituting deflection w in Eq. (50)

$$\frac{d(\nabla^2 \phi)}{dr} = -E_0 \left\{ \frac{f}{r} \left(1 - \frac{r^2}{c^2} \right) \left(-\frac{2r}{c^2} \right) + \frac{1}{R} \left(\frac{dw}{dr} \right) \right\} \quad (54)$$

$$\frac{d(\nabla^2 \phi)}{dr} = -E_0 \left\{ \frac{1}{2r} \left[2f \left(1 - \frac{r^2}{c^2} \right) \left(-\frac{2r}{c^2} \right) \right]^2 + \frac{1}{R} 2f \left(1 - \frac{r^2}{c^2} \right) \left(-\frac{2r}{c^2} \right) \right\} \quad (55)$$

$$\frac{d(\nabla^2 \phi)}{dr} = -E_0 \left\{ \frac{8rf^2}{c^4} \left(1 - \frac{r^2}{c^2} \right)^2 - \frac{1}{R} \frac{4rf}{c^2} \left(1 - \frac{r^2}{c^2} \right) \right\} \quad (56)$$

$$\frac{d(\nabla^2 \phi)}{dr} = -E_0 \left\{ \frac{8f^2}{c^4} \left(r + \frac{r^5}{c^4} - \frac{2r^3}{c^2} \right) - \frac{1}{R} \frac{4f}{c^2} \left(r - \frac{r^3}{c^2} \right) \right\} \quad (57)$$

Integrating above Eq. with respect to r

$$\frac{1}{r} \frac{d}{dr} \left(\frac{rd\phi}{dr} \right) = -E_0 \left\{ \frac{8f^2}{c^4} \left(\frac{r^2}{2} + \frac{r^6}{6c^4} - \frac{r^4}{2c^2} \right) - \frac{1}{R} \frac{4f}{c^2} \left(\frac{r^2}{2} - \frac{r^4}{4c^2} \right) \right\} + c_1 \quad (58)$$

$$\frac{d}{dr} \left(\frac{rd\phi}{dr} \right) = -E_0 \left\{ \frac{8f^2}{c^4} \left(\frac{r^3}{2} + \frac{r^7}{6c^4} - \frac{r^5}{2c^2} \right) - \frac{1}{R} \frac{4f}{c^2} \left(\frac{r^3}{2} - \frac{r^5}{4c^2} \right) \right\} + rc_1 \quad (59)$$

integrating again with respect to r

$$\frac{rd\phi}{dr} = -E_0 \left\{ \frac{8f^2}{c^4} \left(\frac{r^4}{8} + \frac{r^8}{48c^4} - \frac{r^6}{12c^2} \right) - \frac{1}{R} \frac{4f}{c^2} \left(\frac{r^4}{8} - \frac{r^6}{24c^2} \right) \right\} + \frac{r^2 c_1}{2} + c_2 \quad (60)$$

$$\frac{d\phi}{dr} = -E_0 \left\{ \frac{8f^2}{c^4} \left(\frac{r^3}{8} + \frac{r^7}{48c^4} - \frac{r^5}{12c^2} \right) - \frac{1}{R} \frac{4f}{c^2} \left(\frac{r^3}{8} - \frac{r^5}{24c^2} \right) \right\} + \frac{rc_1}{2} + \frac{c_2}{r} \quad (61)$$

Applying boundary condition mentioned in Eq. (45c), which implies $c_2 = 0$.

Now differentiating the Eq. (61) with respect to r

$$\frac{d^2\phi}{dr^2} = -E_0 \left\{ \frac{8f^2}{c^4} \left(\frac{3r^2}{8} + \frac{7r^5}{48c^4} - \frac{5r^4}{12c^2} \right) - \frac{1}{R} \frac{4f}{c^2} \left(\frac{3r^2}{8} - \frac{5r^4}{24c^2} \right) \right\} + \frac{c_1}{2} \quad (62)$$

Now applying boundary condition from Eq. (45b) to evaluate c_1

$$\frac{d^2\phi}{dr^2} - \frac{u}{r} \frac{d\phi}{dr} = 0 \quad (63)$$

Substituting the first and second derivative of stress function ϕ in the above-mentioned Eq.

$$-E_0 \left\{ \frac{8f^2}{c^4} \left(\frac{3r^2}{8} + \frac{7r^5}{48c^4} - \frac{5r^4}{12c^2} \right) - \frac{1}{R} \frac{4f}{c^2} \left(\frac{3r^2}{8} - \frac{5r^4}{24c^2} \right) \right\} + \frac{c_1}{2} + E_0 \left(\frac{\nu}{r} \right) \left\{ \frac{8f^2}{c^4} \left(\frac{r^3}{8} + \frac{r^7}{48c^4} - \frac{r^5}{12c^2} \right) - \frac{1}{R} \frac{4f}{c^2} \left(\frac{r^3}{8} - \frac{r^5}{24c^2} \right) \right\} - \left(\frac{\nu}{r} \right) \frac{rc_1}{2} = 0 \quad (64)$$

$$\frac{E_0 f}{R} \left(\frac{3r^2}{2c^2} - \frac{\nu r^2}{2c^2} - \frac{5r^4}{6c^4} + \frac{\nu r^4}{6c^4} \right) - \frac{2E_0 f^2}{c} \left(\frac{3r^2}{2c^2} - \frac{\nu r^2}{2c^2} + \frac{7r^6}{12c^6} - \frac{\nu r^6}{12c^6} - \frac{5r^4}{3c^4} - \frac{\nu r^4}{3c^4} \right) + (1 - \nu) \frac{c_1}{2} = 0 \quad (65)$$

Substituting $r = c$ and rewriting Eq. (65) as

$$\frac{E_0 f}{R} \left(\frac{2}{3} - \frac{\nu}{3} \right) - \frac{2E_0 f^2}{c} \left(\frac{5}{12} - \frac{11\nu}{12} \right) + (1 - \nu) \frac{c_1}{2} = 0 \quad (66)$$

Now determining the constant c_1

$$c_1 = -\frac{E_0 f^2}{c(1-\nu)} \left(\frac{5}{3} - \frac{11\nu}{3} \right) - \frac{2E_0 f}{R(1-\nu)} \left(\frac{2}{3} - \frac{\nu}{3} \right) \quad (67)$$

Substituting the constant c_1 and c_2 in Eq. (61)

$$\frac{d\phi}{dr} = -E_0 \left\{ \frac{8f^2}{c^4} \left(\frac{r^3}{8} + \frac{r^7}{48c^4} - \frac{r^5}{12c^2} \right) - \frac{1}{R} \frac{4f}{c^2} \left(\frac{r^3}{8} - \frac{r^5}{24c^2} \right) \right\} + \frac{r}{2} \frac{E_0 f^2}{c(1-\nu)} \left(\frac{5}{3} - \frac{11\nu}{3} \right) - \frac{r}{2} \frac{2E_0 f}{R(1-\nu)} \left(\frac{2}{3} - \frac{\nu}{3} \right) \quad (68)$$

$$\frac{d\phi}{dr} = -\frac{E_0 f^2}{6c} \left(\frac{r}{c} \left(\frac{5-11\nu}{1-\nu} \right) - \frac{6r^3}{c^3} + \frac{4r^5}{c^5} - \frac{r^7}{c^7} \right) - \frac{E_0 f c}{R} \left(\frac{2r}{c} \left(\frac{2-\nu}{1-\nu} \right) - \frac{3r^3}{c^3} - \frac{r^5}{c^5} \right) - \frac{prR}{2h} \quad (69)$$

Last component in above Eq. is corresponds to stresses before onset of buckling. Now determining total potential energy of the system. Internal strain energy of mid surface is expressed as

$$U_m = \frac{h}{2E_0} \int_0^c \left[(\nabla^2 \phi)^2 - 2(1+\nu) \frac{1}{r} \frac{d\phi}{dr} \frac{d^2 \phi}{dr^2} \right] 2\pi r dr \quad (70)$$

Substituting derivative of stress function and integrating over the segment area

$$U_m = \frac{\pi(23-9\nu)}{126(1-\nu)} \frac{E_0 h f^4}{c^2} - \frac{\pi(3-\nu)}{9(1-\nu)} \frac{E_0 h f^3}{R} + \frac{\pi(7-2\nu)}{45(1-\nu)} \frac{E_0 h c^4 f^2}{R^2} - \frac{\pi}{3} p R f^2 + \frac{\pi}{3} p f c^2 + \frac{\pi(1-\nu)}{4} \frac{p^2 R^2 c^2}{E_0 h} \quad (71)$$

Internal potential energy of middle surface due to bending is expressed as

$$U_b = \frac{D}{2} \int_0^c \left[(\nabla^2 w)^2 - 2(1+\nu) \frac{1}{r} \frac{dw}{dr} \frac{d^2 w}{dr^2} \right] 2\pi r dr \quad (72)$$

Substituting the derivative of w in above Eq.

$$U_b = \frac{D}{2} \int_0^c \left[\left(\frac{1}{r} \frac{d}{dr} \left(r \frac{dw}{dr} \right) \right)^2 - 2(1+\nu) \frac{1}{r} \frac{dw}{dr} \frac{d^2 w}{dr^2} \right] 2\pi r dr \quad (73)$$

First term in Eq. (73) is evaluated as

$$\nabla^2(w) = \frac{1}{r} \frac{d}{dr} \left(r \frac{dw}{dr} \right) \nabla^2(w) = \frac{1}{r} \frac{d}{dr} \left(r \frac{d}{dr} \left(f \left(1 - \frac{r^2}{c^2} \right)^2 \right) \right) \quad (74)$$

$$\nabla^2(w) = \frac{1}{r} \frac{d}{dr} \left(r 2f \left(1 - \frac{r^2}{c^2} \right) \left(\frac{-2r}{c^2} \right) \right) \quad (75)$$

$$\nabla^2(w) = \frac{-4f}{r} \frac{d}{dr} \left(\frac{r^2}{c^2} - \frac{r^4}{c^4} \right) \quad (76)$$

$$\nabla^2(w) = \frac{-4f}{r} \left(\frac{2r}{c^2} - \frac{4r^3}{c^4} \right) \quad (78)$$

$$\nabla^2(w) = -\frac{8f}{c^2} \left(1 - \frac{2r^2}{c^2} \right) \quad (79)$$

$$\begin{aligned} \frac{d^2w}{dr^2} &= \frac{d^2}{dr^2} \left(f \left(1 - \frac{r^2}{c^2} \right)^2 \right) \frac{d^2w}{dr^2} = -4f \frac{d}{dr} \left(\frac{r}{c^2} - \frac{r^3}{c^4} \right) \frac{d^2w}{dr^2} \\ &= -4f \left(\frac{1}{c^2} - \frac{3r^2}{c^4} \right) \frac{d^2w}{dr^2} = \frac{-4f}{c^2} \left(1 - \frac{3r^2}{c^2} \right) \end{aligned} \quad (80)$$

$$\int_0^c \nabla^2(w) 2\pi r dr = 2\pi \int_0^c r \left(-\frac{8f}{c^2} \left(1 - \frac{2r^2}{c^2} \right) \right)^2 dr \quad (81)$$

$$\int_0^c \nabla^2(w) 2\pi r dr = \frac{128\pi f^2}{c^4} \int_0^c \left(r + \frac{r^5}{c^4} - \frac{2r^3}{c^2} \right) dr \quad (82)$$

$$\int_0^c \nabla^2(w) 2\pi r dr = \frac{128\pi f^2}{c^4} \left[\frac{r^2}{2} + \frac{r^6}{6c^4} - \frac{r^4}{2c^2} \right]_0^c \quad (83)$$

$$\int_0^c \nabla^2(w) 2\pi r dr = \frac{128\pi f^2}{c^4} \left[\frac{c^2}{2} + \frac{c^6}{6c^4} - \frac{c^4}{2c^2} \right] \quad (84)$$

$$\int_0^c \nabla^2(w) 2\pi r dr = \frac{128\pi f^2}{c^4} \left[\frac{c^2}{6} \right] \quad (85)$$

$$\int_0^c \nabla^2(w) 2\pi r dr = \frac{64\pi f^2}{3c^2} \quad (86)$$

Second term in Eq. (73) is evaluated as

$$\int_0^c \left[\frac{1}{r} \frac{d^2w}{dr^2} \frac{dw}{dr} \right] 2\pi r dr = \frac{32\pi f^2}{c^4} \int_0^c \left[r - \frac{4r^3}{c^2} + \frac{3r^5}{c^4} \right] dr \quad (87)$$

$$\int_0^c \left[\frac{1}{r} \frac{d^2w}{dr^2} \frac{dw}{dr} \right] 2\pi r dr = \frac{32\pi f^2}{c^4} \left[\frac{r^2}{2} - \frac{r^4}{c^2} + \frac{r^6}{2c^4} \right]_0^c \quad (88)$$

$$\int_0^c \left[\frac{1}{r} \frac{d^2w}{dr^2} \frac{dw}{dr} \right] 2\pi r dr = \frac{32\pi f^2}{c^4} \left[\frac{c^2}{2} - \frac{c^2}{1} + \frac{c^2}{2} \right] \quad (90)$$

$$\int_0^c \left[\frac{1}{r} \frac{d^2 w}{dr^2} \frac{dw}{dr} \right] 2\pi r dr = 0 \quad (91)$$

$$U_b = \frac{32\pi D}{3} \left(\frac{f}{c} \right)^2 \quad (92)$$

Work of external forces acting on the shell is expressed as mentioned below

$$W = \int_0^c p(w + w_0) 2\pi r dr \quad (93)$$

Here w_0 is pre-buckling deflection and is defined as

$$w_0 = \frac{pR^2}{2E_0 h} (1 - \nu) \quad (94)$$

Substituting w_0 and w in external work Eq. (93)

$$W = \int_0^c p \left(\frac{pR^2}{2E_0 h} (1 - \nu) + f \left(1 - \frac{r^2}{c^2} \right)^2 \right) 2\pi r dr \quad (95)$$

$$W = \frac{\pi p^2 R^2}{E_0 h} (1 - \nu) \int_0^c r dr + 2\pi p f \int_0^c \left[r + \frac{r^5}{c^4} - \frac{2r^3}{c^2} \right] dr \quad (96)$$

$$W = \frac{\pi p^2 R^2}{E_0 h} (1 - \nu) \left[\frac{r^2}{2} \right]_0^c + 2\pi p f \left[\frac{r^2}{2} + \frac{r^6}{6c^4} - \frac{r^4}{2c^2} \right]_0^c \quad (97)$$

$$W = \frac{\pi p^2 R^2}{E_0 h} (1 - \nu) \left[\frac{c^2}{2} \right] + 2\pi p f \left[\frac{c^2}{2} + \frac{c^6}{6} - \frac{c^2}{2} \right] \quad (98)$$

$$W = \frac{\pi p^2 R^2}{E_0 h} (1 - \nu) \left[\frac{c^2}{2} \right] + \pi p f \frac{c^2}{3} \quad (99)$$

$$W = \frac{\pi p^2 R^2 c^2 (1 - \nu)}{2E_0 h} + \frac{\pi}{3} p f c^2 \quad (100)$$

Total potential energy of the system is expressed as

$$\Pi = U_m + U_b - W \quad (101)$$

Substituting U_m , U_b and W from Eqs. (71), (92) and (100) respectively in the above Eq.

$$\begin{aligned} \Pi = & \frac{(23-9\nu)}{126(1-\nu)} \frac{\pi E_0 h f^4}{c^2} - \frac{(3-\nu)}{9(1-\nu)} \frac{\pi E_0 h f^3}{R} + \frac{(7-2\nu)}{45(1-\nu)} \frac{\pi E_0 h c^4 f^2}{R^2} - \frac{\pi}{3} p R f^2 + \\ & \frac{\pi}{3} p f c^2 + \frac{(1-\nu)\pi p^2 R^2 c^2}{4 E_0 h} + \frac{32\pi D}{3} \left(\frac{f}{c}\right)^2 - \frac{\pi p^2 R^2 c^2 (1-\nu)}{2 E h} + \frac{\pi}{3} p f c^2 \end{aligned} \quad (102)$$

Now introducing dimensionless parameter in Eq. (102)

$$\bar{\Pi} = \frac{3}{2} \frac{R}{\pi E_0 h^4} \Pi \quad (103a)$$

$\bar{\Pi}$ is dimensionless potential energy of system in terms of total potential energy, shell radius, shell thickness and equivalent Young's modulus.

$$\bar{\sigma} = \frac{\sigma R^2}{2 E_0 h^2} \quad (103b)$$

$\bar{\sigma}$ is dimensionless stress in terms of membrane stress induced in the shell, shell radius, shell thickness and equivalent Young's modulus.

$$\zeta = \frac{f}{h} \quad (103c)$$

ζ characterizes maximum deflection (Amplitude) of dent forming post buckling.

$$k = \frac{c^2}{R h} \quad (103d)$$

k – characterizes size of the dent. Equation (102) in terms of dimensionless parameter takes the form as

$$\begin{aligned} \bar{\Pi} = & \frac{(23-9\nu)}{84(1-\nu)} \frac{\zeta^4}{k} - \frac{(3-\nu)}{6(1-\nu)} \zeta^3 + \frac{4}{3(1-\nu^2)} \frac{\zeta^2}{k} + \frac{(7-2\nu)}{30(1-\nu)} k \zeta^2 - \bar{\sigma} \zeta^2 - \\ & \frac{3(1-\nu)}{2} k \bar{\sigma}^2 \end{aligned} \quad (104)$$

Now extremizing potential energy of the system in Eq. (104) with respect to variable ζ and k and corresponding stresses are named as $\bar{\sigma}_\zeta$ and $\bar{\sigma}_k$ respectively.

$$\frac{\partial \bar{\Pi}}{\partial \zeta} = 0 \Rightarrow \frac{(23-9\nu)}{21(1-\nu)} \frac{\zeta^3}{k} - \frac{(3-\nu)}{2(1-\nu)} \zeta^2 + \frac{8}{3(1-\nu^2)} \frac{\zeta}{k} + \frac{(7-2\nu)}{15(1-\nu)} k \zeta - 2\bar{\sigma}_\zeta \zeta = 0 \quad (105)$$

Rearranging the above Eq.

$$\bar{\sigma}_\zeta = \frac{1}{2} \left(\frac{(23-6\nu)\zeta^2}{21(1-\nu)k} - \frac{(3-\nu)}{2(1-\nu)}\zeta + \frac{8}{3} \frac{1}{(1-\nu^2)} \frac{1}{k} + \frac{1}{15} \frac{(7-2\nu)}{(1-\nu)} k \right) \quad (106)$$

Now extremizing potential energy of system with respect to k

$$\frac{\partial \bar{\Pi}}{\partial k} = 0 \Rightarrow \frac{(23-9\nu)\zeta^4}{84(1-\nu)k^2} + \frac{4}{3(1-\nu^2)} \frac{\zeta^2}{k^2} - \frac{(7-2\nu)}{30(1-\nu)} \zeta^2 + \frac{3(1-\nu)}{2} \bar{\sigma}_k^2 = 0 \quad (107)$$

Rearranging the above Eq.

$$\bar{\sigma}_k = \left(\frac{2}{3(1-\nu)} \right)^{1/2} \left(\frac{(23-6\nu)\zeta^4}{21(1-\nu)k^2} + \frac{4}{3} \frac{1}{(1-\nu^2)} \frac{\zeta^2}{k^2} + \frac{1}{30} \frac{(7-2\nu)}{(1-\nu)} \zeta^2 \right)^{1/2} \quad (108)$$

$\bar{\sigma}_\zeta$ and $\bar{\sigma}_k$ plotted (Figure 5.8 and Figure 5.9) for various values of k by varying the dimensionless amplitude ζ .

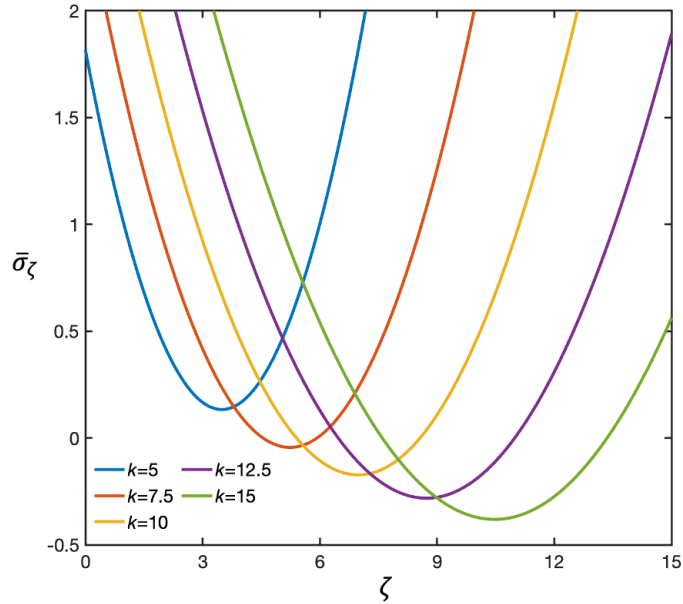


Figure 5.8. Variation of stress $\bar{\sigma}_\zeta$ with respect to ζ for various values of k . The total energy of the system extremized with respect to variable ζ and corresponding stresses are named as $\bar{\sigma}_\zeta$. $\bar{\sigma}_\zeta$ plotted for various values of k by varying the dimensionless amplitude ζ

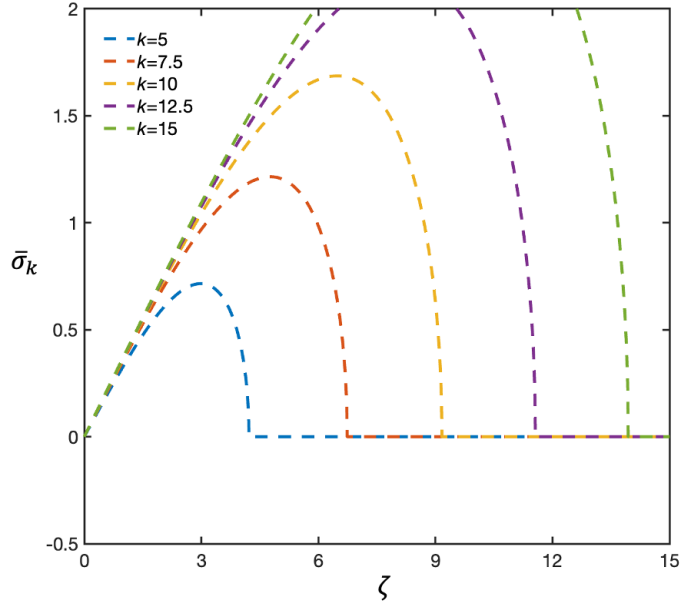


Figure 5.9. Variation of stress $\bar{\sigma}_k$ with respect to ζ for various values of k . The total energy of the system extremized with respect to variable k and corresponding stresses are named as $\bar{\sigma}_\zeta$. $\bar{\sigma}_\zeta$ plotted for various values of k by varying the dimensionless amplitude ζ

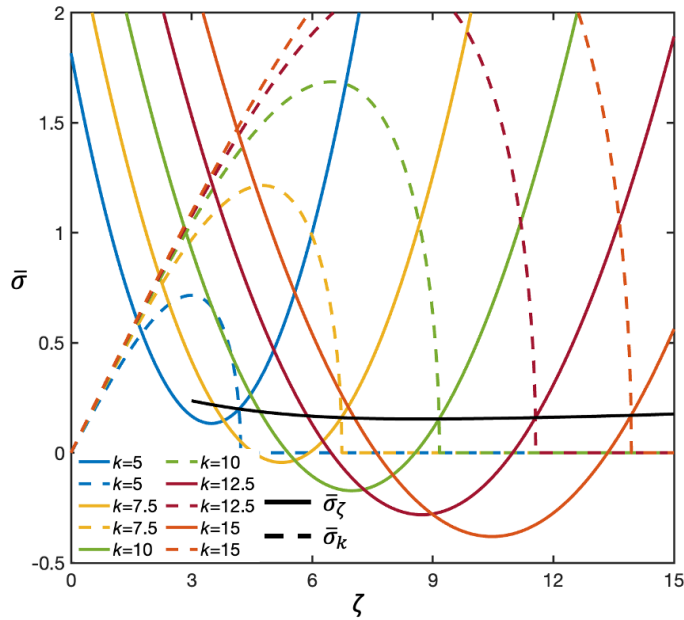


Figure 5.10. Variation of stress $\bar{\sigma}_\zeta$ and $\bar{\sigma}_k$ with respect to ζ for various values of k . The total energy of the system extremized with respect to variable ζ and k and corresponding stresses are named as $\bar{\sigma}_\zeta$ and $\bar{\sigma}_k$ respectively. $\bar{\sigma}_\zeta$ and $\bar{\sigma}_k$ plotted for various values of k by varying the dimensionless amplitude ζ .

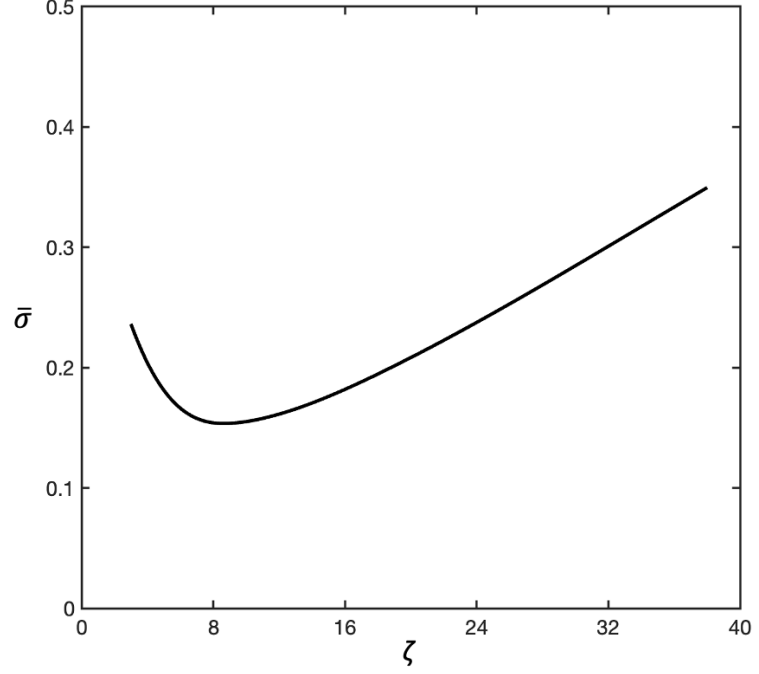


Figure 5.11. Variation of $\bar{\sigma}$ with respect to amplitude (ζ) of displacement w . Resulting curve is locus of points of intersection of curves of $\bar{\sigma}$ after minimization of energy with respect to amplitude ζ of displacement w and k . Minimum stress obtained from curve is termed as critical buckling stress.

$$\bar{\sigma}_c = 0.1548 \text{ at } \zeta = 9.16 \quad (109)$$

Here $\bar{\sigma}_c$ is the critical buckling stress and minima of the curve (Figure 5.11), which is locus of points of intersection of $\bar{\sigma}_\zeta$ and $\bar{\sigma}_k$ (Figure 5.10) plotted for various values of k by varying the dimensionless amplitude ζ . Corresponding critical buckling pressure to critical buckling stress is

$$p_c = 0.3096E_0 \left(\frac{h}{R}\right)^2 \quad (110)$$

Critical buckling pressure by varying the size of circular segment and maximum deflection of shell. Figures (5.12-5.14) shows the deformed shape of droplet.

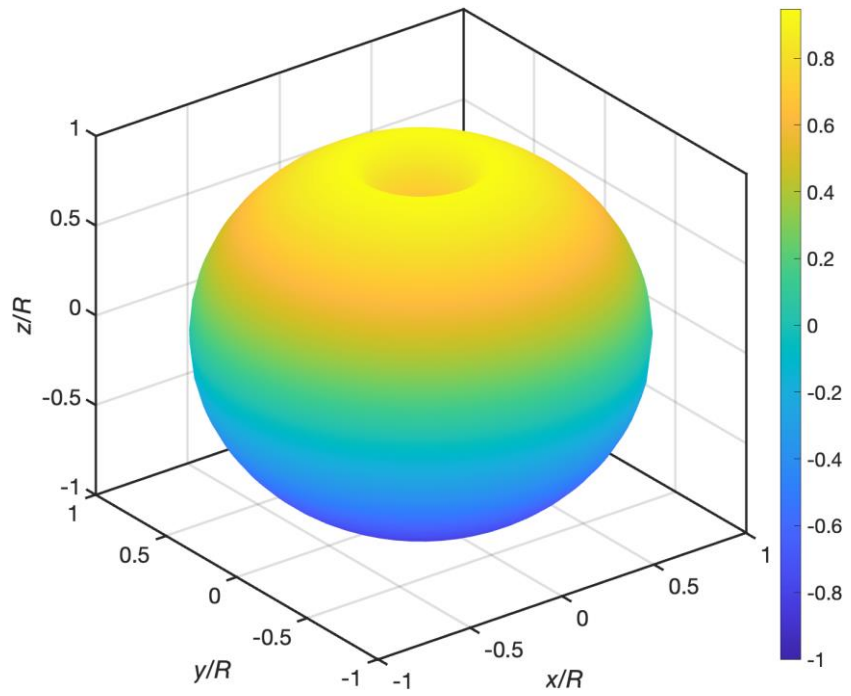


Figure 5.12. Shell in deformed shape post buckling

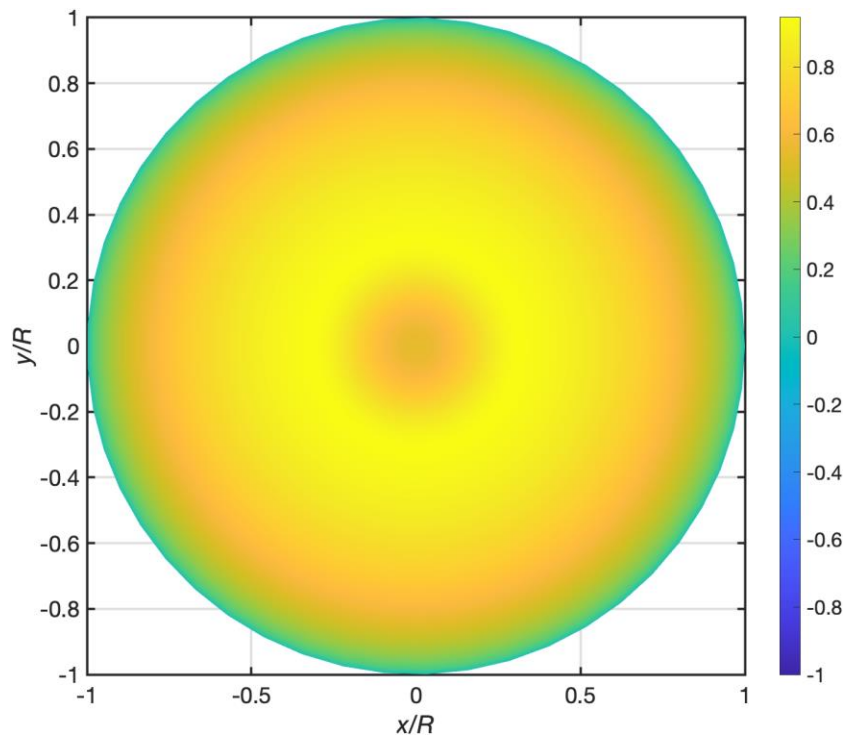


Figure 5.13. Top view of shell in deformed shape post buckling

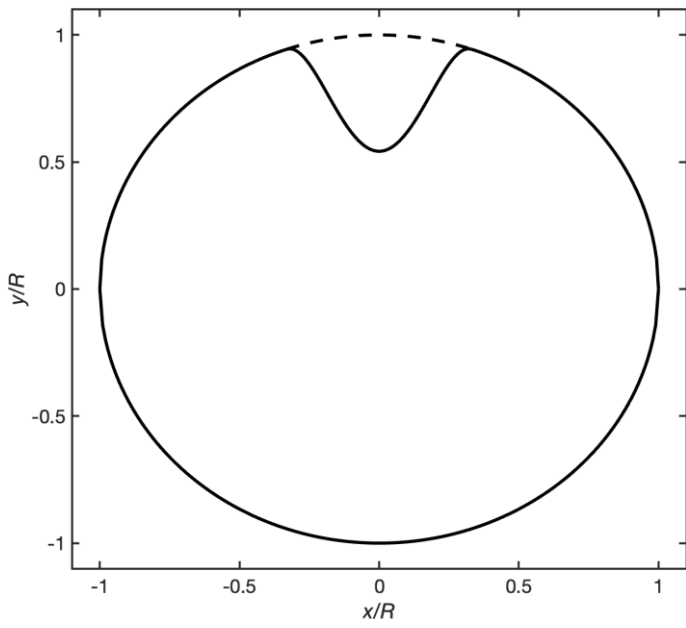


Figure 5.14. 2D cross section of the locally buckled shell structure

Experimental Methods

6.1. Experimental Techniques to Create Spherical Droplet

Generating a spherical droplet is an important aspect for investigating the morphology and drying kinetics of colloidal droplet. To study morphology and buckling behavior of drying droplet of colloidal solution various techniques have been developed and adopted in the literature for creating droplet of required size in controlled environment.

6.1.1. Sessile droplet

A sessile droplet refers to a droplet of liquid that is resting or adhered to a solid surface without spreading. When a droplet of liquid is placed on a solid substrate, several forces come into play that determine its shape and behavior. These forces include gravity, surface tension, adhesion, and cohesion. Surface tension is a cohesive force within the liquid that tends to minimize the surface area of the droplet, causing it to form a spherical or nearly spherical shape. Adhesion refers to the attraction between the liquid molecules and the solid surface, while cohesion refers to the attraction between the liquid molecules themselves. The shape and stability of a sessile droplet depend on the balance between these forces. The contact angle, which is the angle between the solid surface and the droplet's interface, is often used to characterize the shape of a sessile droplet. Placing a droplet at surface which is hydrophobic or superhydrophobic in nature results in nearly spherical shape. When a small volume of liquid is placed over a hydrophobic surface, forces between liquid and substrate surface are repulsive by nature, which helps in forming spherical droplet.

6.1.2. Free flying droplet

A droplet can remain suspended in air by applying an equal force against gravitational force, suspended droplet is known as levitated droplet. Levitated droplet can be achieved by using Leidenfrost effect and standing ultrasound wave.

Leidenfrost effect – droplet remain suspended in air over the vapor of liquid itself. A hot plate having temperature higher than liquid boiling temperature is used to generate the floating droplet.

Acoustic levitation is a fascinating phenomenon that involves using sound waves to suspend and manipulate objects in mid-air. The basic principle behind acoustic levitation is the phenomenon of acoustic radiation pressure. When sound waves propagate through a medium such as air, they create regions of high and low pressure. By carefully controlling the properties of these sound waves, it is possible to create standing waves or resonant conditions where the pressure from the sound waves counteracts the force of gravity, allowing object, such as a small particle or a droplet to float.

6.1.3. Pendent droplet

A pendent droplet refers to a droplet of liquid that is suspended or hanging in air from the tip of filament under controlled environment. When a droplet of liquid is formed and is subjected to gravitational forces, it tends to fall due to gravity. However, under certain conditions, such as when the surface tension of the liquid is strong enough, the droplet can be suspended or hang from a surface or an object. The formation of a pendent droplet depends on the balance between gravity, which pulls the droplet downward, and surface tension, which acts to minimize the surface area of the droplet. The surface tension of the liquid creates an inward force that keeps the droplet compact and prevents it from detaching from the surface.

6.2. Preparation of Aqueous Suspension of Colloid Particles

Colloidal solution or colloid is a stable suspension which is a mixture of nano/micro sized insoluble particles dispersed homogeneously throughout

a solvent of another substance. In this study, a stabilized, diluted dispersion of aqueous Ludox HS-40 nano-silica (from Sigma-Aldrich) with an average particle diameter $d = 12 \pm 2$ nm and dispersity $\mathcal{D} \sim 0.3$ is investigated at different diluted concentration (the buckling behaviour is thus studied only for dilute concentrations). To form a stable, long-term suspension with homogeneously dispersed nanoparticles, the nanosuspension is subjected to ultrasound induced cavitation (sonication) in a RO purified water bath for ~ 15 min.

The volume of the droplets varied between 0.5 and 5 μL which corresponds to spherical drops of 0.49–1.19 mm radius. It is important to note that surface tension (γ_w) plays major role in formation of spherical droplet. Surface tension limit the maximum size of droplet which will remain spherical in shape. Since the capillary length, $l_{cap} = \sqrt{\gamma_w/\rho_w g} = 2.7$ mm, is larger than the drop size, the surface tension dominates gravity resulting in spherical drops. Here, γ_w is the surface tension of water, g is the acceleration due to gravity and ρ_w is the density difference between water and surrounding air.

6.3. Experimental Setup and Procedure

Experimental setup used to perform experiment to study the morphology and buckling behaviour is shown in Figure 6.1. As outlined in the section on experimental techniques, the buckling phenomenon can be investigated by drying aqueous droplets containing suspended particles on a super-hydrophobic surface. In our experiments, a super-hydrophobic surface was prepared by wrapping Teflon tape (0.2 mm thick) on a clean glass slide. In order to study the buckling behaviour of colloidal droplet, The suspension drops were placed via a micro pipette onto the Teflon tape wrapped glass slide. Droplet of colloidal solution subjected to dry at room temperature. Throughout the drying process, a high-resolution camera (Sony α -6100, temporal resolution 0.1833 seconds) combined with a 4.5x Navitar zoom

lens is employed to capture sequential images of the droplet's evolution at various time intervals.

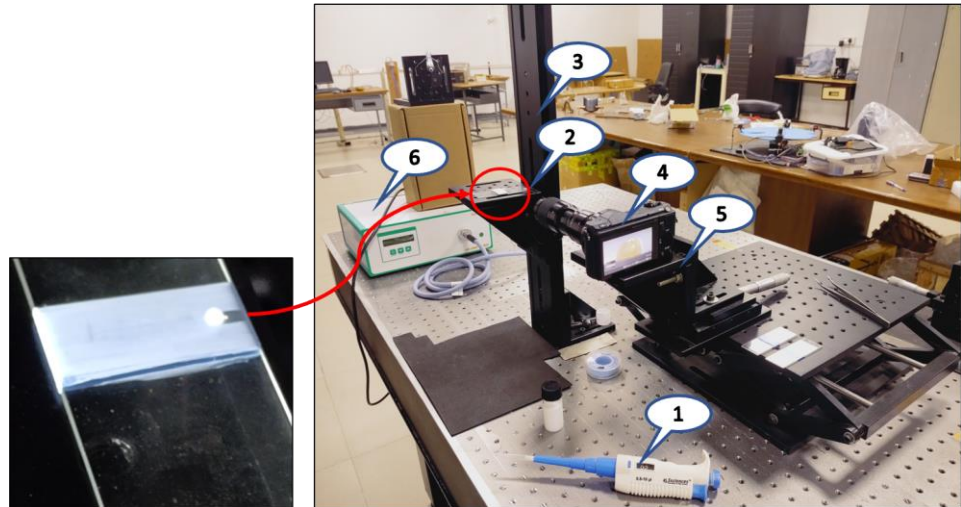


Figure 6.1. Experimental setup showing relative arrangement of different equipment for performing droplet drying experiments.

List of various equipment shown in Figure 6.1 is given below.

- (a) Micropipette
- (b) Teflon wrapped glass slide
- (c) Adjustable height-stand
- (d) Camera (Sony α -6100) with Navitar zoom lens (4.5x zoom)
- (e) Camera stand
- (f) LED light source

Figure 6.2 illustrates the morphological transition of the droplet, exhibiting deformation of the shell caused by the buckling instability.

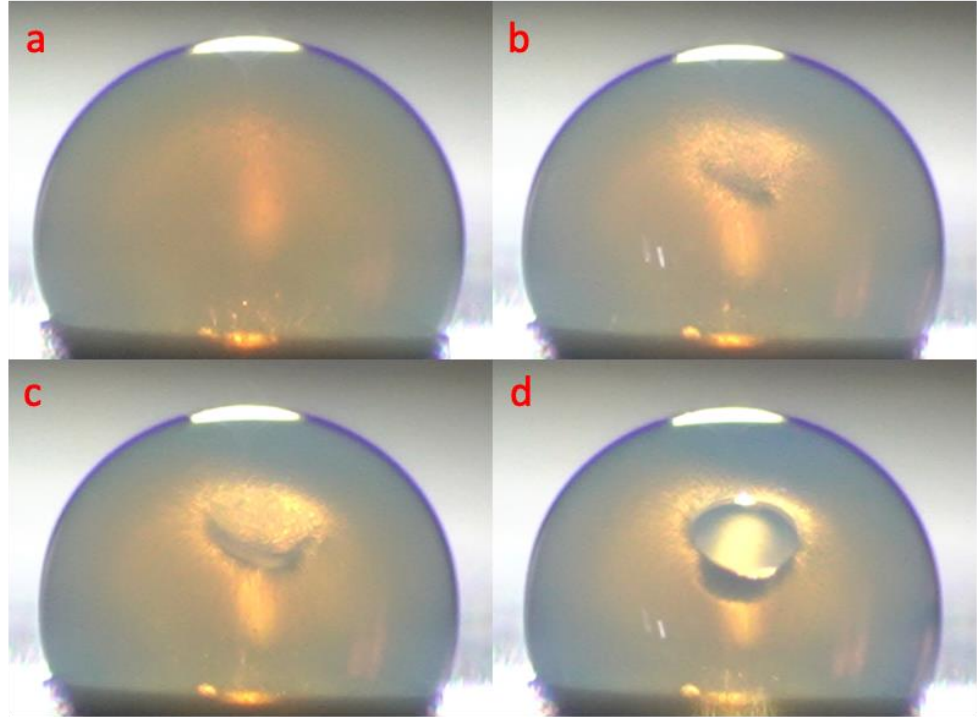


Figure 6.2. Sessile droplet at different stages of drying.

Results and Discussion

In previous section generalized stability analysis performed to understand the buckling behaviour of spherical shell. Following critical parameter are obtained corresponding to onset of buckling from two different analysis approach .

Table 7.1. Comparison of critical parameters evaluated from two different methods.

S. No.	Parameter	Square segment (Pinned joint)	Circular segment (Clamped joint)
1	k	6.4256	10
2	ζ	0.2942	9.16
3	\bar{p}	0.1644	0.3096

Now relating critical buckling pressure with droplet parameter. Substituting E_0 in Eq. (110)

$$p_c = 4.8375 \times 10^{-02} \frac{\phi_{rcp} N G_p}{(1-\nu_p)} \varepsilon_0^{1/2} \left(\frac{h}{R}\right)^2 \quad (111)$$

Here ε_0 , pre buckling strain for thin spherical shell related to pressure by

$$\varepsilon_0 = \frac{h}{2R} p_0/E_0 \quad (112)$$

Evaluating critical strain using relation for pre-buckling strain and upper critical buckling pressure

$$\varepsilon_c = \frac{h}{\sqrt{2}R} \quad (113)$$

Expressing critical buckling pressure in terms of colloid particle packing properties alone

$$p_c = 4.0678 \times 10^{-02} \frac{\phi_{rcp} N G_p}{(1-\nu_p)} \left(\frac{h}{R}\right)^{5/2} \quad (114)$$

Equation (114) relates the critical buckling pressure with properties of particle packing of shell. Equation (114) indicates that critical buckling pressure can be increased by increasing shear modulus of colloid particles i.e., using hard particles.

Critical buckling pressure for colloidal solution (Table 7.1) of water and silica particles studied to know the effect of variation in particle size ($2a$) and droplet size ($2R$). Critical buckling pressure decreases with increasing the droplet size (Figure 7.1). Critical buckling pressure increases with increasing the particle size (Figure 7.2). Droplet with higher particle size is less susceptible to buckling.

Table 7.2. Parameter of colloidal droplet of water and silica particles sample

Parameter	Explanation	Value
ϕ_{rcp}	Random close packing volume fraction	0.64
N	Coordination number	6
G_p	Shear modulus of colloid particle	31 GPa
ν_p	Poisson's ratio of colloid particle	0.17
γ	Surface tension of liquid water interface	0.072 N/m

Now coming to the relation between droplet radius and particle size, if critical thickness (built by random close packing of colloid particles) of the shell, reduced to the size of colloid particle ($2a$), no cracking/buckling of shell occur. Maximum possible capillary pressure is ($5.3 \gamma/a$) in a random close packing of spherical particles of same size [14]. Limiting the critical buckling pressure higher than maximum possible capillary pressure, buckling of shell can be prevented. Corresponding to this relation between particle size and droplet radius for buckling of colloidal droplet is expressed as:

$$\frac{a}{R} \geq 2.45 \left[\frac{\gamma(1-\nu_p)}{\phi_{rcp} N G_p R} \right]^{2/7} \quad (115)$$

Relation between particle size and droplet size in Eq. (115) for buckling of colloidal droplet is compared with experimental results recently published (Figure 7.3 and 7.4) in literature [15]. Here, droplet with different particle size with various droplet radius is subjected to dry and studied for buckling behaviour. On comparing theoretical results with experimental data, theoretical prediction is agreeing well with experimental results.

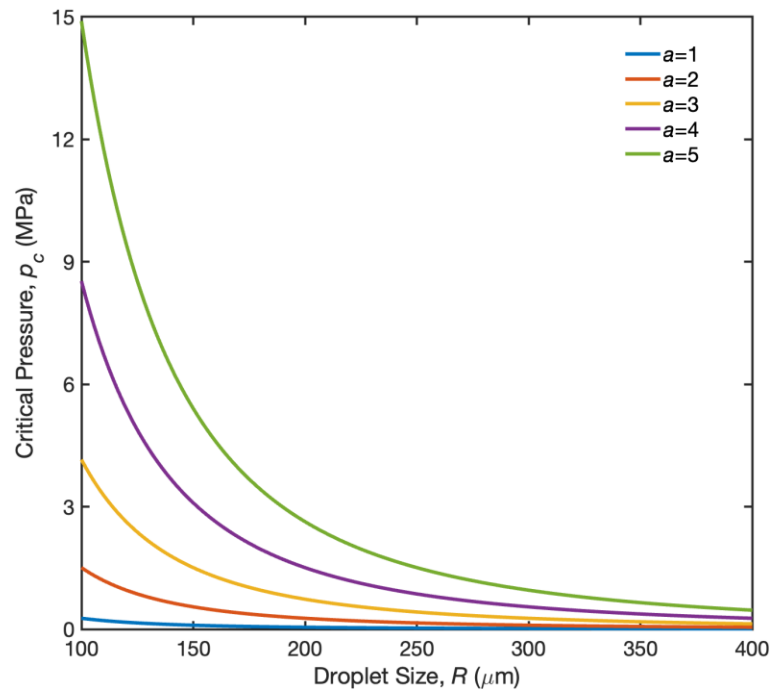


Figure 7.1. Variation of critical pressure (p_c) in respect of droplet size for various colloid particle size. Droplet size and particle size are in same unit (μm) of measurement.

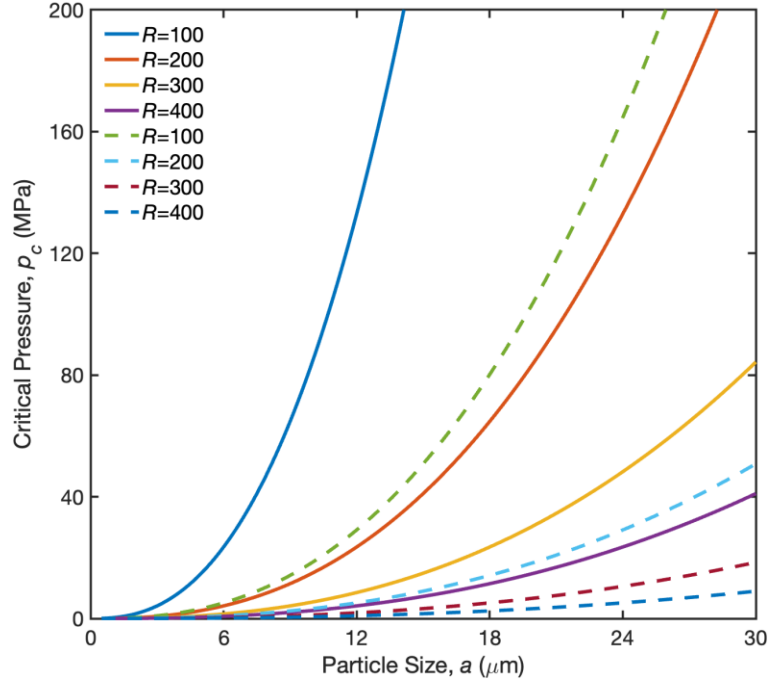


Figure 7.2. Variation of critical pressure (p_c) in respect of colloid particle size for various droplet size. Solid lines are corresponding to upper critical buckling pressure and dashed lines are corresponding to lower critical buckling pressure. Droplet size and particle size are in same unit (μm) of measurement.

For a given droplet radius maximum deflection of dent is function of shell thickness and is directly proportional to thickness. Maximum deflection of shell is 9.16 times thickness of shell.

$$f = 9.16h \quad (116)$$

Critical buckling evaluated above is corresponding to dimensionless parameter $k \sim 10$ (Eq. 91). For a given droplet radius size of the dent size is function of shell thickness and is directly proportional to thickness.

$$k = \frac{c^2}{Rh} \quad (117)$$

Substituting the thickness $h = 2a$ for minimum thickness of monolayer of colloid particles in above Eq. Expression for the size of dent and dent depth amplitude takes the form

$$c \geq \sqrt{20Ra} \quad (118)$$

$$f \geq 18.32a$$

(119)

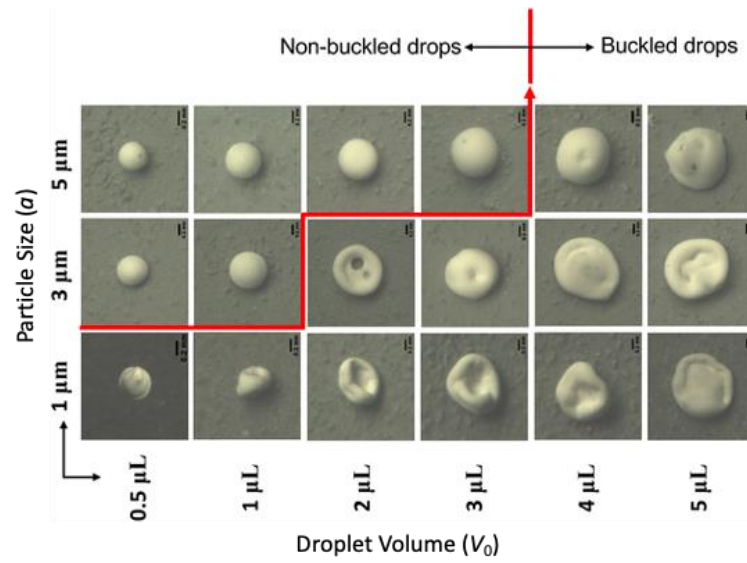


Figure 7.3. Top view of dried granules comprising silica particles with diameters of 1 μm, 3 μm, and 5 μm and with different droplet of volume ranging from 0.5 μL to 5 μL [15].

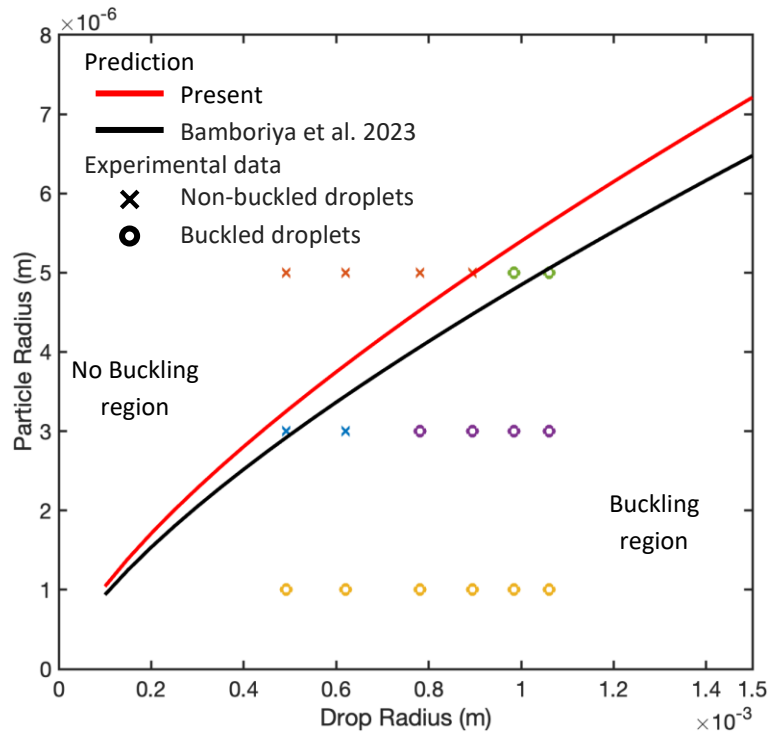


Figure 7.4. Comparison between model prediction and experimental results for dried granules comprising silica particles with diameters of 1 μm , 3 μm , and 5 μm and with different droplet of volume ranging from 0.5 μL to 5 μL as mentioned in Figure 7.3. Here experimental data is represented for various droplet radius corresponding to initial volume mentioned in Figure 7.3.

Conclusion and Future Scope

Stability behaviour of spherical shell of drying colloid particles using theory of shallow shell is investigated. Theoretical analysis to capture the local buckling mechanism is done through considering two different segments, for first case square segment is considered assuming segment to be pin connected with rest of the shell and for second case circular segment is considered assuming segment to be clamped with rest of the shell. The close-form relations are derived for lower critical buckling pressure in terms of colloidal drop shell parameter such as particle size, particle packing volume fraction, particle coordination number and elastic properties of particles and further evolved critical relation for buckling/no buckling, on comparing theoretical results with experimental data, theoretical prediction agreeing well with experimental results. The relationships for size of the dent and dent amplitude in terms of colloid particle size are derived. The results presented here could help in altering the morphology of drying droplet in numerous applications of spray drying process.

This may be stated here that, in the present work stability analysis of colloidal spherical drop is done considering either pin connected or clamped joints, which is not the actual scenario. In real life applications the joints are elastic, which are not considered in this study, and this can be taken up as future studies considering elastic boundary conditions to simulate actual scenario to get improved results.

REFERENCES

- [1] Vehring, R., Foss, W.R. and Lechuga-Ballesteros, D., 2007. Particle formation in spray drying. *Journal of Aerosol Science*, 38(7), pp.728-746.
- [2] Bansal, L., Miglani, A. and Basu, S., 2015. Universal buckling kinetics in drying nanoparticle-laden droplets on a hydrophobic substrate. *Physical Review E*, 92(4), p.042304.
- [3] Tirumkudulu, M.S., 2018. Buckling of a drying colloidal drop. *Soft Matter*, 14(36), pp.7455-7461.
- [4] Tsapis, N., Dufresne, E.R., Sinha, S.S., Riera, C.S., Hutchinson, J.W., Mahadevan, L. and Weitz, D.A., 2005. Onset of buckling in drying droplets of colloidal suspensions. *Physical Review Letters*, 94(1), p.018302.
- [5] Pathak, B. and Basu, S., 2015. Phenomenology and control of buckling dynamics in multicomponent colloidal droplets. *Journal of Applied Physics*, 117(24), p.244901.
- [6] Miglani, A. and Basu, S., 2015. Sphere to ring morphological transformation in drying nanofluid droplets in a contact-free environment. *Soft Matter*, 11(11), pp.2268-2278.
- [7] Pauchard, L., Mermet-Guyennet, M. and Giorgiutti-Dauphiné, F., 2011. Invagination process induced by 2D desiccation of colloidal solutions. *Chemical Engineering and Processing: Process Intensification*, 50(5-6), pp.483-485.
- [8] Lintingre, E., Lequeux, F., Talini, L. and Tsapis, N., 2016. Control of particle morphology in the spray drying of colloidal suspensions. *Soft Matter*, 12(36), pp.7435-7444.
- [9] Boulogne, F., Giorgiutti-Dauphiné, F. and Pauchard, L., 2013. The buckling and invagination process during consolidation of colloidal droplets. *Soft Matter*, 9(3), pp.750-757.

- [10] Paulose, J. and Nelson, D.R., 2013. Buckling pathways in spherical shells with soft spots. *Soft Matter*, 9(34), pp.8227-8245.
- [11] Head, D.A., 2006. Modeling the elastic deformation of polymer crusts formed by sessile droplet evaporation. *Physical Review E*, 74(2), p.021601.
- [12] Eduard S. Ventsel and Krauthammer, T., 2001. *Thin plates and shells: theory, analysis, and applications*. Marcel Dekker.
- [13] Vol'mir, A.S., 1967. *A translation of flexible plates and shells*. Air Force Flight Dynamics Laboratory, Research and Technology Division, Air Force Systems Command, United States Air Force.
- [14] Mason, G. and Mellor, D.W., 1995. Simulation of drainage and imbibition in a random packing of equal spheres. *Journal of Colloid and Interface Science*, 176(1), pp.214-225.
- [15] Bamboriya, O.P. and Tirumkudulu, M.S., 2023. Universality in the buckling behaviour of drying suspension drops. *Soft Matter*, 19(14), pp.2605-2611.